Synthesis and self-assembly of multiblock copolymers with two-length-scale architecture

V.S.D. Voet, M.G. Faber, K. Loos, G. ten Brinke *MSc thesis* **2010**,
Department of Polymer Chemistry, University of Groningen

Synthesis and self-assembly of multiblock copolymers with two-length-scale architecture

V.S.D. Voet, M.G. Faber, K. Loos, G. ten Brinke *MSc thesis* **2010**,
Department of Polymer Chemistry, University of Groningen

Abstract

Multiblock copolymers of polystyrene (PS) and poly(*tert*-butoxy styrene) (P*t*BOS) with a two-length-scale architecture were synthesized through sequential anionic polymerization. The copolymers, with polydispersities between 1.18 and 1.28, are composed of two long end chains and multiple short middle diblock units: PS-*b*-(P*t*BOS-*b*-PS)$_n$-*b*-P*t*BOS. Hydrolysis of this material resulted in the first successful formation of polystyrene-*block*-poly(*para*-hydroxy styrene) (PS-*b*-P*p*HS) multiblock copolymers.

The phase behavior of two dodecablock copolymers (with a different end block length) was investigated, revealing a lamellar morphology for both systems. The limited degree of phase separation is supposedly induced by the short chain length of the middle diblock units (N = 90), and the lamellar structure arises from self-assembly of the end blocks. The scattering pattern of a hexadecablock copolymer indicated nanoscale ordering as well, although phase segregated microdomains were not distinguished in the transmission electron micrographs. The degree of microphase separation is low, due to the large number of middle diblock units (n = 7) in combination with their short chain length (N = 90).

Esterification of PS-*b*-P*p*HS resulted in polystyrene-*block*-poly(*para*-trifluoroacetoxy styrene) (PS-b-P*p*TFAS) multiblock copolymers. The aromatic ester moieties in the copolymers were found to be unstable, and are thought to undergo UV radiation induced rearrangement. Nonetheless, the phase behavior of the converted copolymers was still investigated. The degree of microphase separation was not improved compared to the PS-*b*-P*p*HS system, and similar repeating distances were determined.

A unique two-length-scale lamellar morphology with multiple periodicity was observed for an octablock copolymer consisting of longer middle diblock units (N = 180). The hierarchical

nanostructure includes one thick lamellar domain of PS, another thick lamellar domain of P*p*HS, and two thin lamellae of PS and P*p*HS in between, all in excellent agreement with the two-length-scale architecture of the multiblock copolymer. The repeating unit of the large length scale was determined to be 44 nm, although the degree of long-range order was limited.

An alternative lamellar-in-lamellar structure was observed for a tetrablock copolymer, obtained through premature termination during anionic polymerization. This morphology consists of thick lamellae of PS with three thin lamellar domains of P*p*HS and PS in between, in agreement with the two-length-scale molecular architecture. The large length scale period was calculated to be 40 nm. Due to the broader molecular weight distribution, the degree of long-range order was low.

Contents

1. General introduction

1.1. Block copolymer phase behavior

Block copolymers are macromolecules composed of two or more covalently bonded polymers which are chemically distinct. In general, chemically distinct homopolymers are immiscible and phase separation readily occurs. However, when two homopolymer chains are covalently linked to form a block copolymer, macrophase separation is impossible because both blocks are part of the same macromolecule. Instead, the immiscible blocks demix at the nanoscale with the disparate polymer chains stretched away from the interface that is formed at their juncture. The balance between enthalpic interfacial energy between the blocks and entropic chain stretching energy of the individual blocks, as described in the Gibbs free energy of mixing ΔG_{mix} (Equation 1), gives rise to microphase separation. Due to their ability to microphase separate, block copolymer systems are suitable for a wide range of applications in nanotechnology: from nanoelectronics and photonics[1,2] to controlled drug delivery[3].

$$\frac{\Delta G_{mix}}{k_b T} = \frac{f_A}{N_A}\ln(f_A) + \frac{f_B}{N_B}\ln(f_B) + f_A f_B \chi_{AB}$$

Equation 1. ΔG_{mix} is the Gibbs free energy of mixing, k_B is the Boltzmann constant, T is the temperature of the system, f_A and f_B are the compositions of block A and B respectively, N_A and N_B are the block lengths of block A and B respectively and χ_{AB} is the interaction parameter.

The self-assembly of block copolymers in the melt results in periodic structures with characteristic length scales of the order of ten to hundreds of nanometers. The phase separation on nanoscale is dependent on variables such as chain architecture, temperature and block lengths. While the most basic chain architecture is a linear block copolymer, more complicated structures like graft, cyclic and star copolymers are also possible, as are dendritic and hyperbranched, and combinations thereof.

Microphase separation of block copolymers occurs below the order-disorder transition temperature (ODT). On the other hand, the order-order transition temperature (OOT) describes the transition of one morphology into another. In the Flory-Huggins theory[4,5]

[1] Scherf, U.; Gutacker, A.; Koenen, N. *Acc. Chem. Res.* **2008**, *41*, 1086.
[2] Paquet, C.; Kumacheva, E. *Materials Today* **2008**, *11*, 48.
[3] Yokoyama, M.; Miyauchi, M.; Yamada, N.; Okano, T.; Sakurai, K.; Kataoka, K.; Lnoue, S. *J. Controlled Release* **1990**, *11*, 269.
[4] Huggins, M.L. *J. Chem. Phys.* **1941**, *9*, 440.

temperature dependence is expressed in the dimensionless interaction parameter χ_{AB}, describing the interactions between copolymer blocks A and B (Equation 2). A higher Flory-Huggins interaction parameter means more unfavorable interactions between both blocks.

$$\chi_{AB} \equiv \frac{z\Delta\varepsilon}{k_B T}$$

Equation 2. χ_{AB} is the interaction parameter, z is the number of nearest neighbor monomers, k_B is the Boltzmann constant, $\Delta\varepsilon$ is the energy difference between contacts A-A, B-B and A-B and T is the temperature of the system.

The phase diagram for a phase segregating block copolymer is determined both by χN and composition parameter f, which is the volume fraction of one of the blocks. Symmetrical volume fractions ($f \sim 0.5$) result in a lamellar morphology, while high (or low) volume fractions result in isolated spheres in a matrix of the other component. In between, cylindrical and gyroidal morphologies are observed.

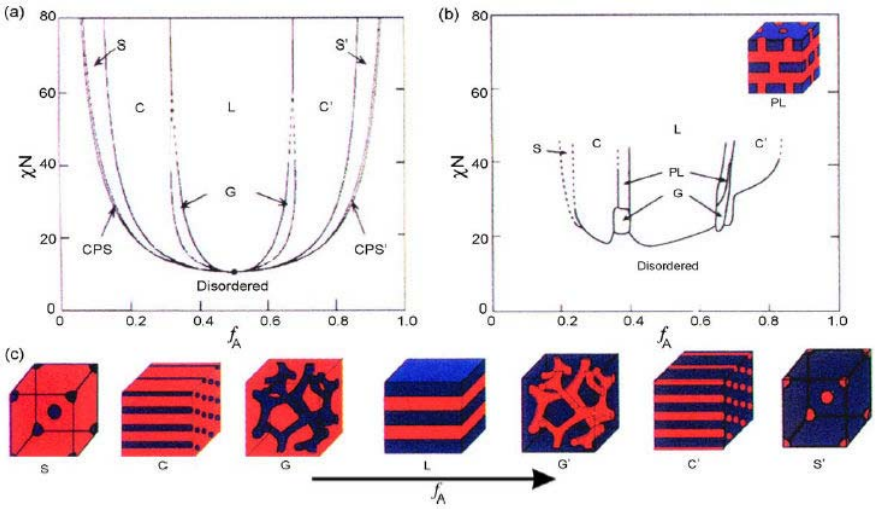

Figure 1. Phase diagrams for linear AB diblock copolymers, comparing theory and experiment (ref. 6).

The phase diagram for linear diblock copolymers[6] was calculated by self-consistent mean-field theory[7,8] and predicts four different morphologies: Spherical (S), Cylindrical (C), Gyroid (G) and Lamellar (L), depending on the composition f_A, interaction parameter χ and chain

[5] Flory, P.J. *J. Chem. Phys.* **1941**, *9*, 660.
[6] Bates, F.S.; Fredrickson, G.H. *Physics Today* **1999**, *52*, 32.
[7] Matsen, M.W.; Schick, M. *Phys. Rev. Lett.* **1994**, *72*, 2660.
[8] Matsen, M.W.; Bates, F.S. *Macromolecules* **1996**, *29*, 1091.

length N (Figure 1). The right diagram is based on experimental results from polystyrene-*block*-polyisoprene diblock copolymers[9]. This less symmetric experimental phase diagram introduces also the perforated lamellar morphology (PL). Complete mixing is observed for $\chi \cdot N < 20$.

1.1.1. Diblock copolymers of polystyrene and poly(para-hydroxy styrene)

Apart from self-organization in the bulk, block copolymers can also form micelles in dilute solutions when a selective solvent[10] (selective to one block) is used. Self-assembly of block copolymers in solution will lead to the formation of micelles, containing a core of insoluble or less soluble blocks and a swollen corona of soluble blocks. Usually, the driving force of this micellization is the repulsive interaction between insoluble blocks and the selective solvent. Typical structures such as spheres and rod- or disk-like micelles are observed. These micellar nanostructures attracted a considerable amount of attention in the past few years due to their use as drug carriers in delivery systems[11], as templates for nanotechnology[12] and in separation technologies[13].

Linear diblock copolymers consisting of polystyrene and poly(*para*-hydroxy styrene) gain special interest due to their self-associative hydrogen bonding capability of the hydroxyl styrene moieties. It turns out that the formation of hydrogen bonds is an additional driving force to obtain micelle formation in block copolymer solutions. Zhao *et al.*[14] synthesized polystyrene-*block*-poly(*para*-[*tert*-butyldimethylsilyl]oxy styrene) through a living anionic polymerization, followed by desilylation to obtain the desired amphiphilic polystyrene-*block*-poly(*para*-hydroxy styrene) (PS-*b*-P*p*HS). Cylindrical micelles, having a diameter around 40 nm and lengths of 300 nm were observed with static and dynamic light scattering experiments.

More recently, Tung *et al.*[15] discussed the micellar morphologies of amphiphilic polystyrene-*block*-poly(*para*-hydroxy styrene) at various concentrations in acetone. They synthesized polystyrene-*block*-poly(*tert*-butoxy styrene) (PS-*b*-P*t*BOS) through sequential anionic polymerization, and hydrolysis led to PS-*b*-P*p*HS block copolymer. When block copolymer

[9] Kandpur, A.K.; Förster, S.; Bates, F.S.; Hamley, I.W.; Ryan, A.J.; Bras, W.; Almdal, K.; Mortensen, K. *Macromolecules* **1995**, *28*, 8796.
[10] Tuzar, Z.; Kratochvil, P. *Adv. Colloid Interface Sci.* **1976**, *6*, 201.
[11] Torchilin, V.P. *J. Controlled Release* **2001**, *73*, 137.
[12] Ding, J.; Liu, G. *Macromolecules* **1997**, *30*, 655.
[13] Hurter, P.N.; Hatton, T.A. *Langmuir* **1992**, *8*, 1291.
[14] Zhao, J.Q.; Pearce, E.M.; Kwei, T.K.; Jeon, H.S.; Kesani, P.K.; Balsara, N.P. *Macromolecules* **1995**, *28*, 1972.

micelles were prepared in acetone, which is a good solvent for hydroxy styrene, worm-like and sunflower-like morphologies were obtained, consisting of a polystyrene core and a poly(hydroxy styrene) corona. To investigate the importance of self-associative hydrogen bonding in these systems, micelles from the prepolymer PS-*b*-P*t*BOS in acetone were prepared for comparison. The different hydrogen interaction abilities of both block copolymers resulted in the formation of distinct micellar morphologies. Furthermore, the strength of self-associative hydrogen bonding in the PS-*b*-P*p*HS/acetone system was decreased by adding a small amount of poly(4-vinylpyridine), and resulted in the formation of other micellar morphologies.

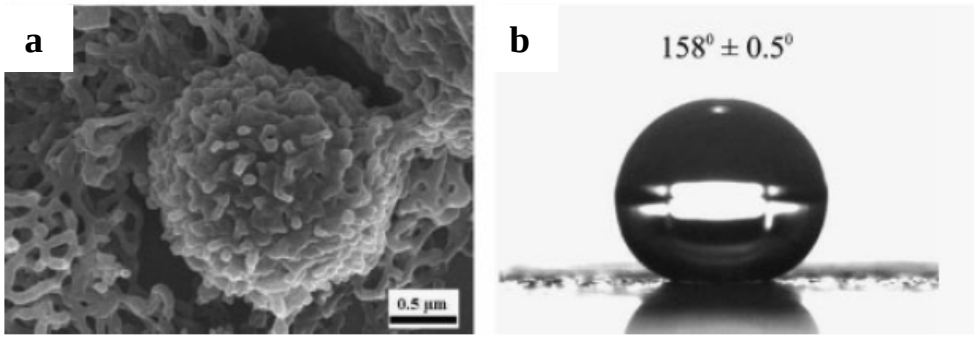

Figure 2. (a) SEM image of pincushion-like micelles formed by PS-*b*-P*p*HS in a THF/toluene mixture. (b) Contact angle of water droplet on a surface of [a] (ref. 16).

Tung *et al.*[16] also studied micellization of the same diblock copolymers in THF/toluene mixtures. Several crew-cut micelles were obtained (like porous spheres and pincushion-like aggregates) by changing the selective solvent content or the initial concentration. The wettability of block copolymer films containing these crew-cut aggregates was investigated. A smooth surface of PS-*b*-P*p*HS is moderately hydrophobic (θ=90°), however the hydrophobicity of a pincushion-like micellar aggregated film (Figure 2) is greatly enhanced due to the increase in surface roughness (θ=158°). Such dramatic water repellency behavior is called superhydrophobic behavior.

Yoshida *et al.*[17] reported micelle formation of nonamphiphilic diblock copolymers, adding a good solvent for both blocks. They proposed another approach to synthesize PS-*b*-P*p*HS,

[15] Tung, P-H., Kuo, S-W.; Chen, S-C.; Lin, C-L.; Chang, F-C. *Polymer* **2007**, *48*, 3192.
[16] Tung, P-H., Kuo, S-W.; Chan, S-C.; Hsu, C-H.; Wang, C-F.; Chang, F-C. *Macromol. Chem. Phys.* **2007**, *208*, 1823.
[17] Yoshida, E.; Kunugi, S. *Macromolecules*, *35*, 6665.

through living radical polymerization mediated by 4-methoxy-TEMPO[18]. As expected, no micelle formation was observed in 1,4-dioxane, which is a good solvent for both PS and P*p*HS. However, after addition of 1,4-butanediamine (BDA: H_2N-$(CH_2)_4$-NH_2), micellization occurred through hydrogen bond cross-linking between the P*p*HS blocks (Scheme 1), demonstrated by ^{1}H-NMR analysis.

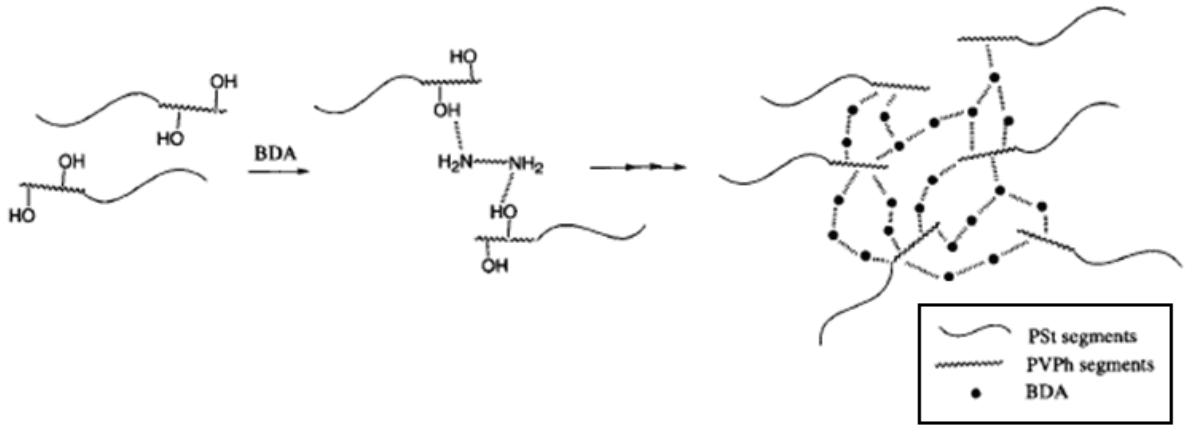

Scheme 1. Hydrogen bond cross-linking between the P*p*HS blocks induced by BDA, resulting in micellization (ref. 17).

1.2. Self-assembly of triblock copolymers

The situation becomes more complex when dealing with block copolymers consisting of more than two blocks. In case of ABC triblock copolymers, three distinct Flory-Huggins interaction parameters (χ_{AB}, χ_{BC} and χ_{AC}) and three block fractions (f_A, f_B and f_C) are involved. Various morphologies can be formed due to the increased number of parameters that may be varied. Furthermore, the block sequence is strongly influencing the system as well. The most important morphologies were determined theoretically[6,19] (Figure 3), and several of them are also proven experimentally[20,21].

[18] Yoshida, E.; Kunugi, S. *J. Polym. Sci., Polym. Chem. Ed.* **2002**, *40*, 3063.
[19] Zheng, W.; Wang, Z-G. *Macromolecules* **1995**, *28*, 7215.
[20] Gobius du Sart, G.; Rachmawati, R.; Voet, V.; Alberda van Ekenstein, G.; ten Brinke, G.; Loos, K. *Macromolecules* **2008**, *41*, 6393.
[21] Gobius du Sart, G. *Zernike Institute PhD Thesis,* University of Groningen, Groningen **2009**.

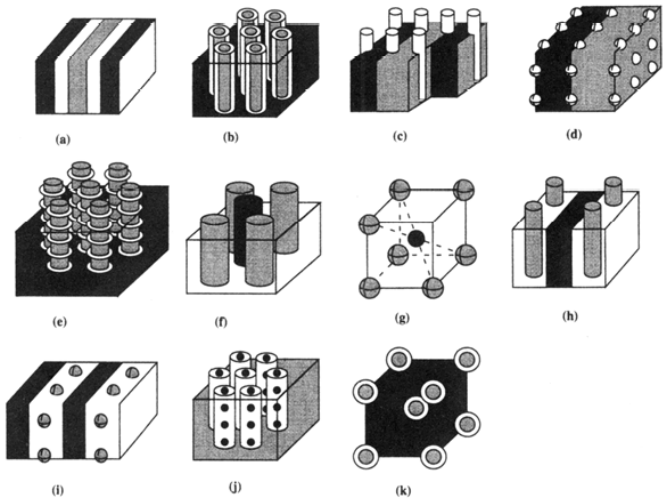

Figure 3. Schematic representation of linear ABC triblock copolymer morphologies, determined theoretically (ref. 19).

A decade ago, Bailey *et al.*[22] suggested to distinguish triblock copolymers according to the typical frustration in the system, caused by the ratio between the three interaction parameters. For example, when the Flory-Huggins parameter describing the interaction between block A and C (χ_{AC}) is large compared to the other two χ-parameters (χ_{AB} and χ_{BC}), a system with no frustration (F^0) is obtained. Typically, morphologies such as triple lamellae, alternating spheres and alternating cylinders were found[23] (Figure 4).

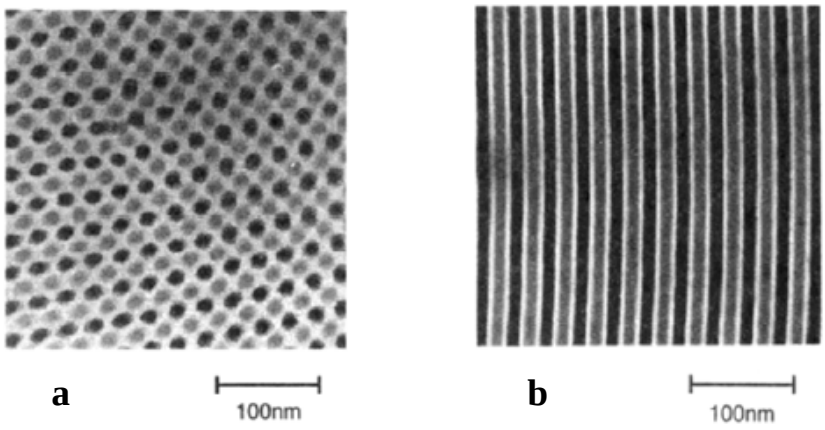

Figure 4. (a,b) TEM images of polyisoprene-*block*-polystyrene-*block*-poly-2-vinylpyridine) triblock copolymers stained with OsO_4, showing an alternating cylindrical morphology [a] and a triple lamellar morphology [b] (ref. 23).

[22] Bailey, T.S.; Pham, H.D.; Bates, F.S. *Macromolecules* **2001**, *34*, 6994.
[23] Mogi, Y.; Nomura, M.; Kotsuji, H.; Ohnishi, K.; Mutsushita, Y. And Noda, I. *Macromolecules* **1994**, *27*, 6755.

On the other hand, when χ_{AC} is smaller than one (F^1), or even both (F^2) of the remaining two χ-parameters, the triblock copolymer system is called frustrated. In this case, the interface between block A and C is not anymore the most unfavorable one. Interesting morphologies were discovered while investigating these systems, such as core-shell cylinders, core-shell gyroid, cylinders-between-lamellae and rings- or helices-around-cylinders. For example, Stadler *et al.*[24] were able to synthesize polystyrene-*block*-polybutadiene-*block*-poly(methyl methacrylate) and polystyrene-*block*-poly(ethylene-*co*-butylene)-*block*-poly(methyl methacrylate), and self-assembly of these triblock copolymers resulted in cylinders-between-lamellae and rings-around-cylinders.

In addition to linear ABC triblock copolymers, microphase separation of block copolymer systems with an alternative topology, such as ABC star-type triblock copolymers in which all three blocks are joined together, is also well-studied in the literature. Self-assembly of such systems usually results in the formation of so-called Archimedean tiling patterns[25] (Figure 5).

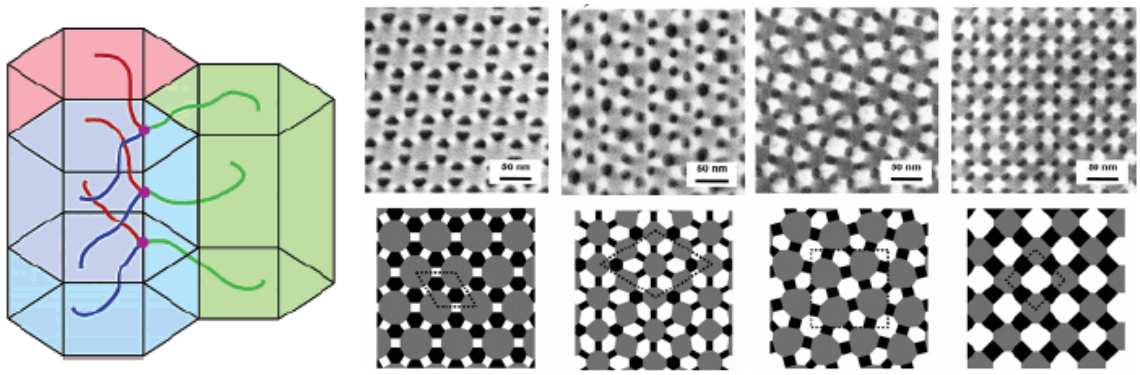

Figure 5. (left) Schematic review of self-assembly of an ABC star-type triblock copolymer. (right) TEM images and corresponding schematics of four Archimedean tiling patterns for star-type polyisoprene-*block*-polystyrene-*block*-poly-2-vinylpyridine (ref. 25).

1.3. Multiblock copolymers with two-length-scale architecture

From di- and triblock copolymers, it is a small step towards discussing tetra-, hexa- or dodecablock copolymer, also called multiblock copolymers. Theoretical models were introduced to predict phase separation behavior of linear multiblock copolymers having

[24] Stadler, R.; Auschra, C.; Beckmann, J.; Krapper, U.; Voight-Martin, I.; Leibler, L. *Macromolecules* **1995**, *28*, 3080.
[25] Matsushita, Y. *Macromolecules* **2007**, *40*, 771.

various architectures, and several morphologies such as lamellae, cylinders and gyroid were found to be stable[26,27].

Self-assembly of multiblock copolymers of the type $(AB)_n$, with constant block lengths, was studied experimentally by Matsushita[28] and Smith[29,30] at the same time. Polystyrene-*block*-polyisoprene ($(SI)_n$ type) multiblock copolymers with nearly equal block lengths were synthesized via a multistep monomer addition technique using sequential anionic polymerization. Alternating lamellar nanostructures were observed, as expected for strongly segregated symmetric copolymers. They both concluded from TEM and SAXS data, that the lamellar domain spacing decreases with an increasing number of blocks, i.e. D decreases with increasing n. This suggests that the middle blocks contract the microdomains in perpendicular direction with respect to the lamellae, driven by the ability of these middle blocks to adopt either the bridge or loop conformation. In addition, a more recent study from Spontak *et al.*[31] discussed the increase of tensile modulus E and yield stress σ with increasing n.

Wu *et al.*[32] reported a bridge-to-loop transition in shear aligned lamellar morphology heptablock copolymers consisting of polystyrene and polyisoprene. The multiblock copolymers were synthesized through anionic copolymerization, using a bifunctional coupling agent to couple tetrablocks, ending up with heptablocks. Different processing conditions (shear and strain) were applied during rheology experiments, showing the ability to drive the transformation from a predominantly bridged to a looped conformation.

The formation of nanostructures in block copolymer melts usually involves one characteristic length scale and self-assembly of these systems results in the classical morphologies as discussed above. However, more complex morphologies can also be achieved by block copolymers with a two-length-scale molecular architecture. Self-assembly of such systems leads to the formation of hierarchical structures having multiple periodicity.

Nap *et al.*[33] presented a detailed simulation of microphase separation of $A(BA)_n$ type multiblock copolymers, where block lengths of the $(BA)_n$ block sequence are considerably shorter than the A end block. At elevated temperatures, diblock phase separation was found between the large end block and the smaller multiblock sequence. However, reducing the temperature resulted in a lamellar-in-lamellar morphology.

---

[26] Benoit, H.; Hadziioannou, G. *Macromolecules* **1988**, *21*, 1449.
[27] Matsen, M.W.; Schick, M. *Macromolecules* **1994**, *27*, 6761.
[28] Matushita, Y.; Mogi, Y.; Mukai, H.; Watanabe, J.; Noda, I. *Polymer* **1994**, *35*, 246.
[29] Smith, S.D.; Spontak, R.J.; Satkowski, M.M.; Ashraf, A.; Lin, J.S. *Phys. Rev. B* **1993**, *47*, 14555.
[30] Smith, S.D.; Spontak, R.J.; Satkowski, M.M.; Ashraf, A.; Heape, A.K.; Lin, J.S. *Polymer* **1994**, *35*, 4527.
[31] Spontak, R.J.; Smith, S.D. *J. Polym. Sci. B: Polym. Phys.* **2001**, *39*, 947.
[32] Wu, L.; Lodge, T.; Bates, F.S. *Macromolecules* **2004**, *37*, 8184.

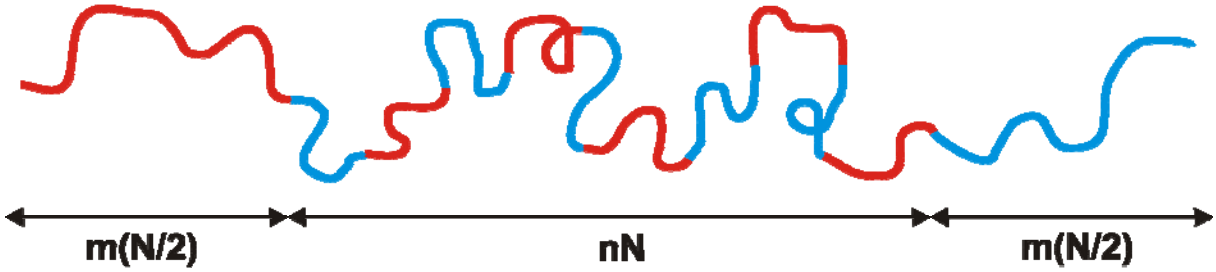

Figure 6. Schematic view of the molecular two-length-scale architecture of the symmetric multiblock copolymer $A_{m(N/2)}$-*b*-($B_{N/2}$-*b*-$A_{N/2}$)$_n$-*b*-$B_{m(N/2)}$.

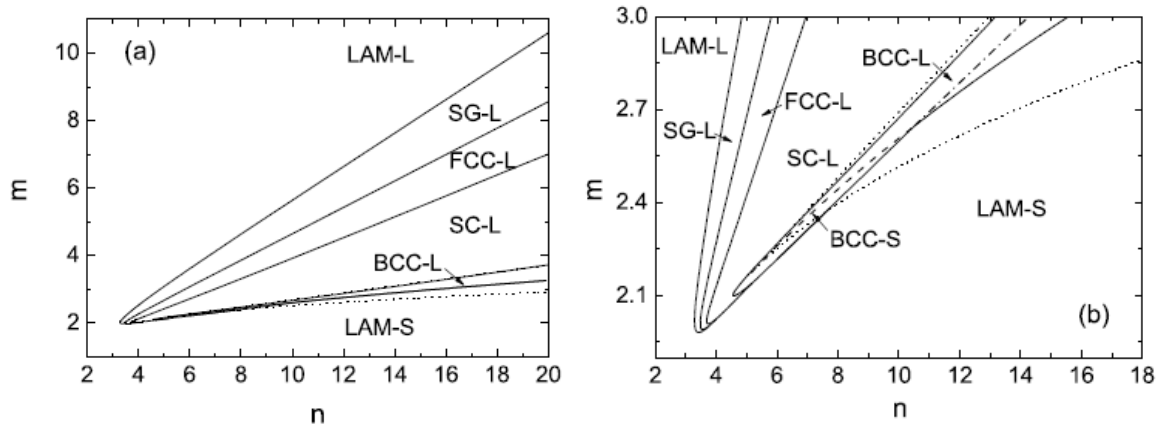

Figure 7. Phase diagrams in (*n*,*m*)-plane of $A_{m(N/2)}$-*b*-($B_{N/2}$-*b*-$A_{N/2}$)$_n$-*b*-$B_{m(N/2)}$ multiblock copolymers (ref. 34).

Another theoretical study of Smirnova *et al.*[34,35] focused on phase behavior of a special class of multiblock copolymers with a two-length-scale architecture: A_{fmN}-*b*-($B_{N/2}$-*b*-$A_{N/2}$)$_n$-*b*-$B_{(1-f)mN}$. Herein is *n* the number of middle diblock units, *N* the size of one middle diblock, *m* is the relative total length of end blocks with respect to the middle diblock units and parameter *f* characterizes the asymmetry ratio between the end blocks. For symmetric multiblock copolymers f = 0.5 applies, resulting in the architecture $A_{m(N/2)}$-*b*-($B_{N/2}$-*b*-$A_{N/2}$)$_n$-*b*-$B_{m(N/2)}$ (Figure 6). One length scale is related to the size of the diblock *N* the other to the total size of the block copolymer. Phase behavior of such block copolymer melts was studied within the weak segregation theory[36,37]. In the critical point, several ordered phases were found, such as conventional lamellar (LAM), body-centered cubic (BCC), face-centered cubic (FCC), simple cubic (SC) and single gyroid (SG) morphology, depending on the structural parameters *n* and *m*. The resulting phase diagram in the (*n*,*m*)-plane shows the predicted morphologies (Figure

[33] Nap, R.; Sushko, N.; Erukhimovich, I.; ten Brinke, G. *Macromolecules* **2006**, *39*, 6765.
[34] Smirnova, Y.G. *MSC PhD Thesis,* University of Groningen, Groningen **2006**.
[35] Smirnova, Y.G.; ten Brinke, G.; Erukhimovich, I.Y. *J. Chem. Phys.* **2006**, *124*, 54907.
[36] Leibler, L. *Macromolecules* **1980**, *13*, 1602.
[37] Fredrickson, G.; Hefland, E. *J. Chem. Phys.* **1987**, *87*, 697.

7). The presence of the two lamellar morphologies LAM-L(arge) and LAM-S(mall), both with a distinct periodicity, illustrates the influence of the two-length-scale architecture.

Nagata *et al.*[38] were the first to report a hierarchical lamellar-in-lamellar nanostructure, arising from self-assembly of well-designed multiblock copolymers. They synthesized a two component undecablock copolymer through sequential anionic polymerization, consisting of two long polystyrene (S) end blocks and nine short middle blocks with alternating polyisoprene (I) and polystyrene (S) chains: S-$(IS)_4$I-S. Self-assembly of this copolymer was studied with TEM and SAXS, and a complex lamellar nanostructure with multiple periodicity was observed, composed of one thick lamellar domain consisting of long polystyrene chains and three thin lamellar domains consisting of short middle blocks (Figure 8a). The latter suggests that the short chains favor looped over bridged conformation. This material, showing multiple periodicity, is thought to find application as a photochromic crystal.

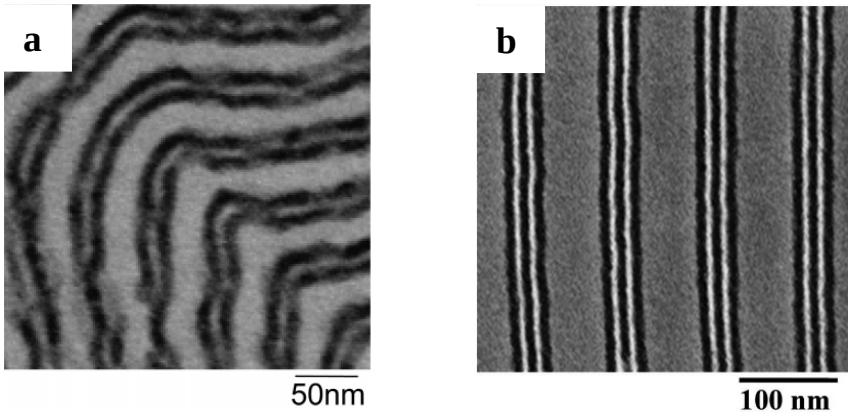

Figure 8. (a) TEM image of S-$(IS)_4$I-S undecablock copolymer stained with OsO_4, showing a hierarchical lamellar-in-lamellar nanostructure (ref. 38). (b) TEM image of P-$(IS)_4$I-P undecablock copolymer stained with OsO_4 and I_2 to illustrate a three component double periodicity lamellar structure with high degree of orientation (ref. 39).

Another striking example of multiblock copolymer self-assembly resulting in nanostructures with two intrinsic length scales was published by Masuda *et al.*[39]. An three component undecablock copolymer, including two long poly(2-vinylpyridine) (P) end blocks and nine short middle blocks consisting of alternating polyisoprene (I) and polystyrene (S) chains, shortly denoted as P-$(IS)_4$I-P, was synthesized. Phase separation in the bulk was analyzed by TEM, showing a parallel double periodicity structure of which the degree of lamellar orientation is high and the long-range order is excellent. The nanostructure includes one thick

[38] Nagata, Y.; Masuda, J.; Noro, A.; Cho, D.; Takano, A.; Matsushita, Y. *Macromolecules* **2005**, *38*, 10220.

lamellar domain of poly(2-vinylpyridine) (gray) and five thin lamellae, consisting of three polyisoprene (black) and two polystyrene (white) microdomains (Figure 8b).

An alternative approach to produce complex two-length-scale structures, was demonstrated by Ruokolainen *et al.*[40,41]. They observed hierarchical structure-in-structure morphologies by investigating a blend system of pentadecylphenol (PDP) with polystyrene-*block*-poly(4-vinylpyridine), thereby introducing noncovalent bonded intermolecular interactions. Due to the hydrogen bonding between PDP and P4VP, a two-length-scale periodicity was observed (Figure 9). Interesting photonic and electronic properties are ascribed to this material, due to the temperature sensitivity of the hydrogen bonds defining the short-length-scale lamellar ordering[42].

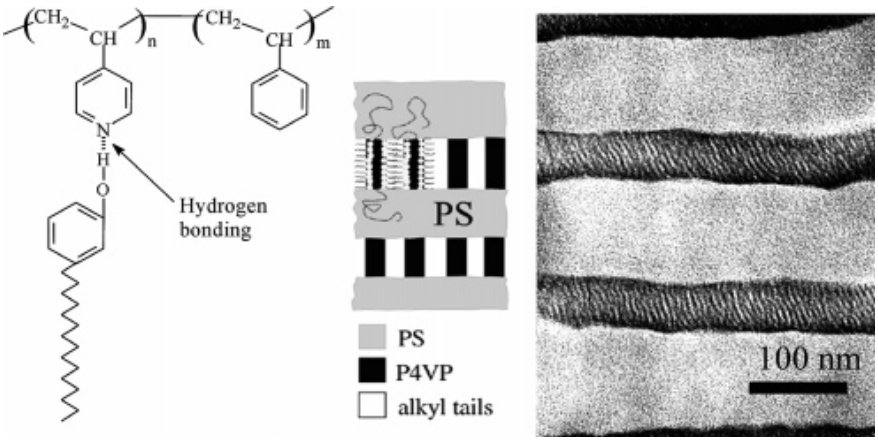

Figure 9. Hierarchical structure-in-structure lamellar morphology of PS-*b*-P4VP / PDP blend (ref. 25).

1.4. Sequential anionic polymerization

The preparation of block copolymers used to study phase behavior requires a controlled synthesis to obtain a product with narrow polydispersity. As discussed in the previous sections, a common approach of synthesizing (multi)block copolymers is by sequential anionic polymerization[43]. This so-called living polymerization was first studied by Michael Szwarc and his co-workers in 1956[44,45]. They investigated the polymerization of styrene in

[39] Masuda, J.; Takano, A.; Nagata, Y.; Noro, A.; Matsushita, Y. *Phys. Rev. Lett.* **2006**, *97*, 98301.
[40] Ruokolainen, J.; Mäkinen, R.; Torkkeli, M.; Mäkelä, T.; Serimaa, R.; Ten Brinke, G.; Ikkala, O. *Science* **1998**, *280*, 557.
[41] Ruokolainen, J.; Ten Brinke, G.; Ikkala, O. *Adv. Mater.* **1999**, *11*, 777.
[42] Valkama, S.; Kosonen, H.; Ruokolainen, J.; Torkkeli, M.; Serimaa, S.; Ten Brinke, G.; Ikkala, O. *Nat. Mater.* **2004**, *3*, 872.
[43] Szwarc. M.; *J. Pol. Sci. A: Pol. Chem.* **1998**, *36*, ix.
[44] Szwarc. M.; Levy, M.; Milkovich, R. *J. Am. Chem. Soc.* **1956**, *78*, 2656.

THF using sodium naphtalenide as initiator, and concluded that the degree of termination and chain transfer is negligible. Moreover, the resulting polymer chains retain their ability to propagate and grow to a desired size, and were therefore referred as living polymers. The polymerization proceeds until all monomer is consumed, and continues after the addition of new monomers to the reaction, i.e. sequential living anionic polymerization provides synthetic control of the block sequence and length. This makes anionic polymerization such a favorable technique for producing well-defined block polymers.

1.4.1. Characteristics of living polymerizations

In a subsequent publication, Waack *et al.*[46] proved that the number average degree of polymerization P_n is given by a simple relation (Equation 3). Since the number of growing chains in a living anionic polymerization is constant and all monomer is consumed, the degree of polymerization is equal to the ratio between initial monomer and initial initiator concentration. According to this equation, the molecular weight of polymers synthesized through anionic polymerization can be regulated in a reliable way.

$$\overline{P_n} = \frac{[M]_0}{[I]_0}$$

Equation 3. P_n is the number average degree of polymerization, $[M]_0$ is the initial monomer concentration and $[I]_0$ is the initial initiator concentration.

As was predicted by Flory[47] more than fifteen years before the invention of living anionic polymerization by Szwarc, polymerizations free of termination and chain transfer result in a Poisson distribution, i.e. a narrow molecular weight distribution with a polydispersity *PDI* close to 1 (monodispers) for high molecular weights (Equation 4). Indeed, many studies on anionic polymerizations reported polydispersities below 1.05.

$$PDI = 1 + 1/\overline{P_n}$$

Equation 4. *PDI* is polydispersity and P_n is the number average degree of polymerization.

[45] Szwarc. M. *Nature* **1956**, *178*, 1168.
[46] Waack, R.; Rembaum, A.; Coombes, J.D.; Szwarc, M. *J. Am. Chem. Soc.* **1957**, *79*, 2026.

1.4.2. Initiation, propagation and termination

The polymerization usually starts with a fast initiation using organometal compounds such as organolithium as the initiator. Initiation needs to be fast compared to propagation in order to reach a narrow molecular weight distribution. As an example, the initiation of styrene by *sec*-butyl lithium is depicted (Scheme 2), showing the formation of a styrene anion. Alternative monofunctional initiators are $NaNH_2$, alkoxides and cyanides. In addition, bifunctional initiators may be used as well, such as the earlier discussed sodium naphtalenide[44]. The number average degree of polymerization now relates to the ratio $[M]_0 / ½[I]_0$. Polyfunctional initiators like 1,3,5-tris(α-methoxybenzyl)benzene (TMBB) were investigated to yield star-shaped polymers[48].

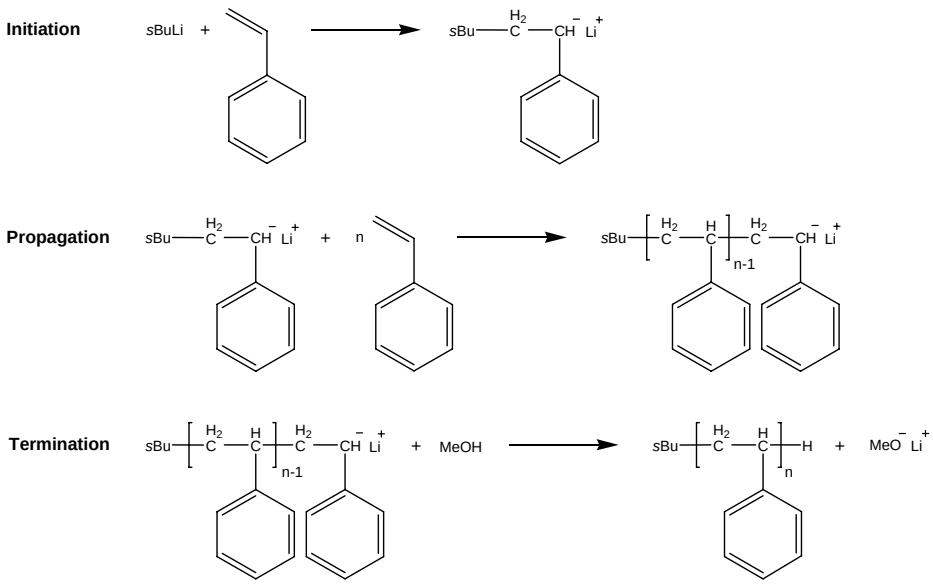

Scheme 2. Initiation, propagation and termination of (poly)styrene, using *sec*-butyl lithium as initiator and methanol as terminating agent.

An anionic polymerization can propagate via the sequential addition of monomers to the anionic chains (Scheme 2). Electron withdrawing substituents stabilize this propagating anionic chain end. On the other hand, acidic protons will terminate the reaction, thus functionalities such as carboxylic acids and alcohols need to be protected. Moreover, the reaction should be free of O_2, since molecular oxygen will lead to oxidative coupling of chain ends. The polymerization can be carried out in both polar (tetrahydrofuran, dimethylether) and non-polar solvents (hexanes, benzene).

---

[47] Flory, P.J. *J. Am. Chem. Soc.* **1940**, *62*, 1561.
[48] Fujimoto, T.; Tani, S.; Takano, K.; Ogawa, M.; Nagasawa, M. *Macromolecules* **1978**, *11*, 673.

To eventually end the controlled living polymerization, terminating agents are added to the system, since the active anionic polymer chain ends will not terminate through combination or disproportionation mechanisms. Particularly effective terminators are proton donors like methanol (Scheme 2) and ethanol. The possibility to choose your terminating agent, allows the selective introduction of functional end groups (thiols, ethers, alkyns) by adding a specific linking agent[49]. The use of bifunctional linking agents can facilitate the coupling of two active chains, resulting in high molecular weight polymers[32,50].

1.5. Small-angle X-ray scattering (SAXS)

In 1895 the German physicist Wilhelm Röntgen discovered X-rays, i.e. Röntgen rays. A few years later, Max von Laue described the diffraction of these X-rays by crystals[51]. Both received the Noble Prize in Physics in 1901 and 1914 respectively, reflecting the great importance of their work. Nowadays, X-ray diffraction is a powerful technique for structure determination.

To study structures with sizes in the order of 10 Å or larger, such as block copolymer nanostructures having segregated microdomains, small-angle X-ray scattering (SAXS) is a powerful tool[52]. Indeed, the intensity of scattered X-rays on block copolymer samples contains a lot of information at small angles. The scattering pattern of an irradiated sample, containing block copolymer microphase separated domains with different electron densities, provides characteristic data about the morphology.

Diffraction results from the scattering of X-rays by electrons in the sample and interference of the scattered waves. The scattering geometry (including beam direction and wavelength) is characterized by the scattering vector q (Equation 5).

$$q = \frac{4\pi \sin\theta}{\lambda}$$

Equation 5. q is the scattering vector, θ is the Bragg angle (angle between incident ray and scattering plane) and λ is the wavelength.

[49] Hirao, A.; Hayashi, M. *Acta Polym.* **1999**, *50*, 219.
[50] Bellas, V.; Rehahn, M. *Macromol. Rapid Comm.* **2007**, *28*, 1415.
[51] Atkins, P.; de Paula, J. *Atkins' Physical Chemistry,* Oxford University Press, Oxford **2002**.
[52] Roe, R-J. *Methods of X-ray and Neutron Scattering in Polymer* Science, Oxford University Press, New York **2000**.

Bragg's Law (Equation 6), developed by William Bragg together with his son Lawrence, describes the relation between the order of reflection, the wavelength, the interplanar spacing (representing the period of repetition) and the so-called Bragg angle, which is half the scattering angle 2θ. For small-angle X-ray scattering, the scattering angle is typically less than 2°.

$$n\lambda = 2D\sin\theta$$

Equation 6. Bragg's Law: n is an integer (1,2,3,…), λ is the wavelength, D is the spacing between planes in the lattice and θ is the Bragg angle.

Combining these equations results in a relation between the interplanar spacing and the scattering vector (Equation 7) for n = 1, meaning the first-order of reflection. Thus, the microdomain spacing of block copolymers can easily be calculated when the scattering vector of the first-order peak is determined.

$$D = 2\pi/q$$

Equation 7. D is the spacing between planes in the lattice and q is the scattering vector.

In practice, the peaks in a SAXS pattern are broad due to imperfections present in the block copolymer nanostructure and the limited domain size of local ordering. As a consequence, usually only the first reflections are visible as separated peaks. As discussed earlier, scattering patterns provide characteristic information about the block copolymer morphology. For example, the ratio between the scattering peaks and the first-order peak in a pattern representing a lamellar morphology[53] is 1:2:3:4 etc. (Figure 10). The scattering is dependent on the unit cell and lattice planes of the nanostructure, described by the so-called Miller indices h, k and l (Equation 8).

[53] Gobius du Sart, G.; Vucovic, I.; Alberda van Ekenstein, G.; Polushkin, E.; Loos, K.; ten Brinke, G. *Macromolecules* **2010**, *43*, 2970.

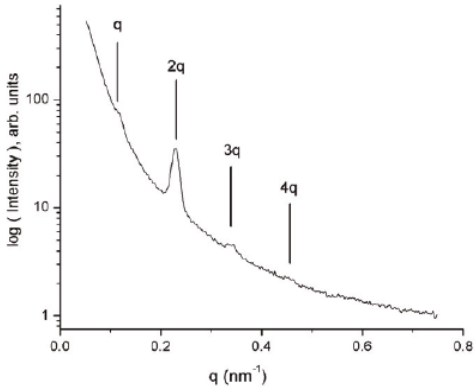

Figure 10. SAXS intensity profile of a triblock copolymer supramolecular complex: P*t*BOS-*b*-PS-*b*-P4VP(PDP) (ref. 53).

$$a) \qquad q(hkl) = q_1 h$$

$$b) \qquad q(hkl) = q_1 \sqrt{h^2 + k^2 + l^2}$$

$$c) \qquad q(hkl) = q_1 \sqrt{h^2 + hk + k^2}$$

Equation 8. *q(hkl)* is the scattering vector, q_1 is the first-order scattering vector and *h*, *k* and *l* are the miller indices. a) Lamellae, b) Spheres and c) Cylinders.

1.6. Transmission electron microscopy (TEM)

In 1931 Max Knoll and Ernst Ruska developed the first electron microscope and generated magnified images of mesh grids. This device consisted of two magnetic lenses to achieve higher magnifications. Eight years later, the first commercial transmission electron microscope was built.

Transmission electron microscopes are the electron optical instruments analogue to conventional light microscopes. TEM measurements are performed in vacuum, since air scatters the illuminated electrons. Due to the short wavelengths of electrons, high resolution around 5 Å can be achieved. The maximum resolution *d* is described by Abbe's equation (Equation 9)[54] and depends on the wavelength of electrons and the so-called numerical aperture.

$$d = \frac{0.61\lambda}{NA}$$

Equation 9. *d* is the resolution, λ is the electron wavelength and *NA* the numerical aperture: $n \cdot \sin(\alpha)$.

[54] Sawyer, L.C.; Grubb, D.T. *Polymer Microscopy*, Chapman and Hall, London **1987**.

Electrons are emitted thermally by heating a filament, usually made of tungsten. This tungsten filament functions as the cathode, having a high negative potential in the order of 100 kV. The electron beam accelerates towards the anode and is then focused by magnetic lenses. Subsequently, the electron beam hits the specimen and electrons are scattered. When performing transmission electron microscopy, the transmitted electrons pass through multiple lenses to focus and enlarge the image, and are finally projected onto a fluorescent screen or CCD camera. Contrast in a TEM image arises from scattering by the specimen instead of absorption. Regions that contain heavy elements (with a high atomic number) appear dark in the image, since the elastic scattering predominates inelastic scattering.

Due to the ability to create images with high resolution, TEM is a powerful technique to study block copolymer nanostructures with microdomain sizes in the order of a few Ångström or larger. However, most copolymers are composed of low atomic number elements, resulting in low contrast images due to little variation in electron density. To improve contrast, staining agents composed of heavy elements may be added to selectively stain a block by either a chemical interaction or selective physical absorption, in order to increase the electron density difference and thus the contrast. The investigated sample is usually an ultra thin microtomed section of a block copolymer film, placed on a mesh grid.

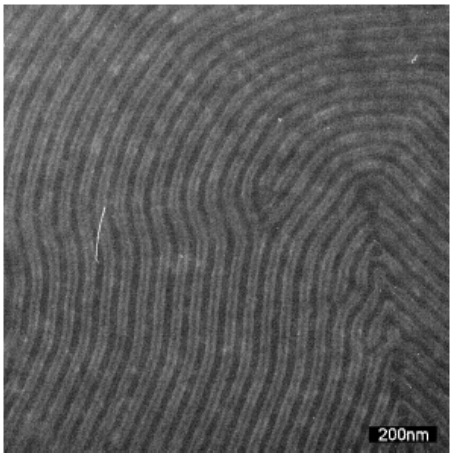

Figure 11. TEM image of a triblock copolymer supramolecular complex: P*t*BOS-*b*-PS-*b*-P4VP(PDP), stained with I_2 and RuO_4 (ref. 53).

Popular staining agents are osmium tetroxide, ruthenium tetroxide and iodine[55]. OsO_4 may stain unsaturated hydrocarbons, alcohols, ethers, amines. In addition, RuO_4 also stains aromatics, such as styrene. Due to the high vapor pressure of both compounds, staining in the

[55] Thomas, E.L. *Structure of Crystalline Polymers*, Elsevier, London **1984**.

gaseous phase is favorable: a method called vapor staining. To reveal the morphology in triblock copolymer systems consisting of three components, a combination of staining agents can be used as well (Figure 11).

1.7. Project description

In summary, the phase behavior of various block copolymer systems, and particularly that of multiblock copolymers with two intrinsic length scales, was outlined in this introduction. In addition, methods of synthesis and analysis were discussed: sequential anionic polymerization, small-angle X-ray scattering and transmission electron microscopy.

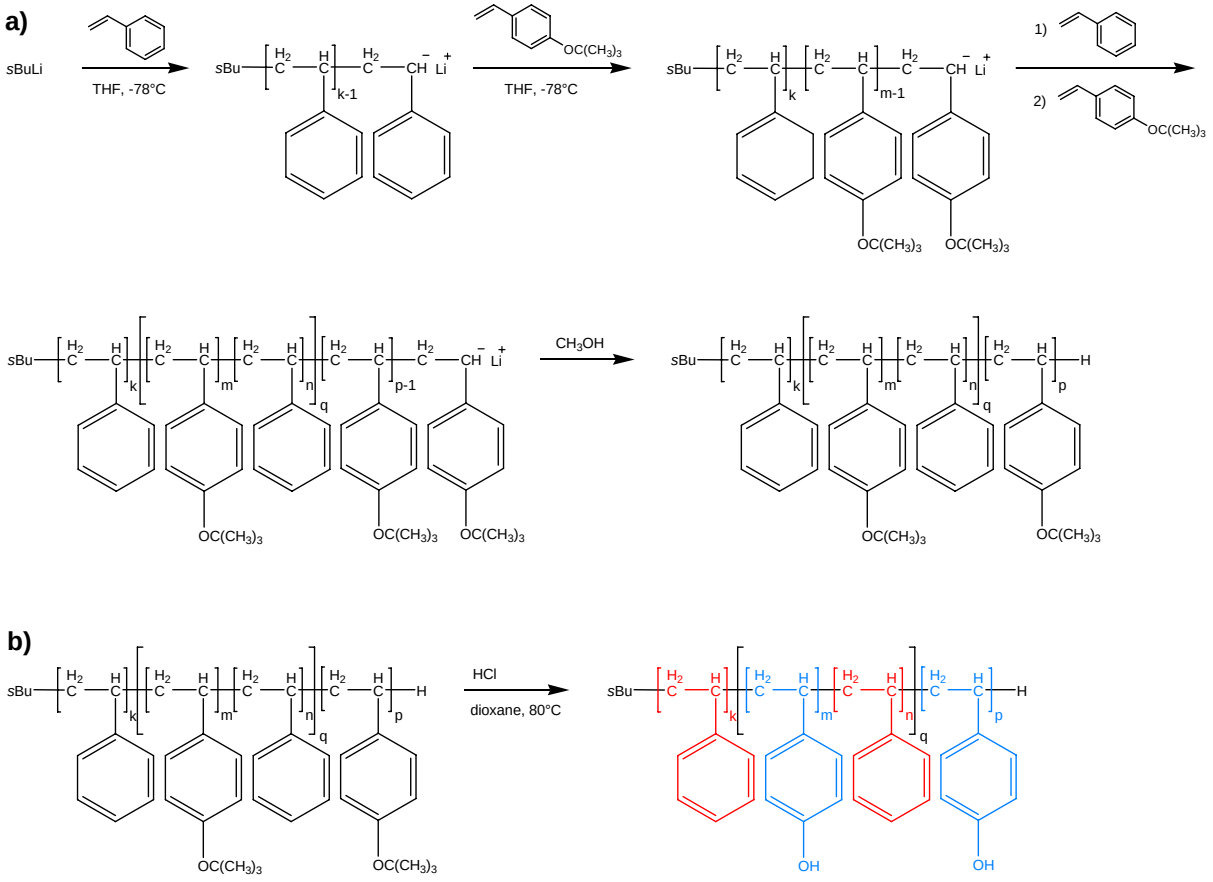

Scheme 3. (a) Sequential anionic polymerization of styrene and *tert*-butoxy styrene. (b) Hydrolysis to obtain polystyrene-*block*-poly(*para*-hydroxy styrene) multiblock copolymer.

The aim of this thesis is to synthesize and characterize a two-length-scale multiblock copolymer system as described theoretically by Smirnova *et al.*[34,35], consisting of polystyrene and poly(hydroxy styrene). The synthesis can be performed through sequential living anionic

polymerization in THF at -78 °C with *sec*-butyl lithium as initiator, introducing styrene and *tert*-butoxy styrene as monomers, both able to polymerize subsequently (Scheme 3a). The desired polystyrene-*block*-poly(*para*-hydroxy styrene) multiblock copolymer is obtained through acidic cleavage of the *tert*-butoxy groups[16,56] (Scheme 3b). The block copolymer phase behavior of the resulting product will be analyzed by SAXS and TEM.

The Flory-Huggins χ-parameter of styrene and tert-butoxy styrene is small, as determined by a random copolymer study ($0.031 < \chi_{S,tBOS} < 0.034$)[21]. However, the interaction parameter of styrene and *para*-hydroxy styrene is assumed to be higher ($\chi_{S,pHS} \approx 0.25$)[57], and therefore it is believed that the phase behavior of PS-*b*-P*p*HS multiblock copolymers (with two intrinsic length scales) is worthwhile to study.

Unfortunately, this system seems to be unstable when heated above 130 °C, probably due to partial condensation cross-linking of the phenol groups[58]. On the other hand, the glass transition of P*p*HS is considerably higher ($T_g \approx 180$ °C). Therefore, it is not possible to obtain self-organization when cooling down from the melt. However, self-assembly of the multiblock copolymers can be achieved by solvent-casting instead.

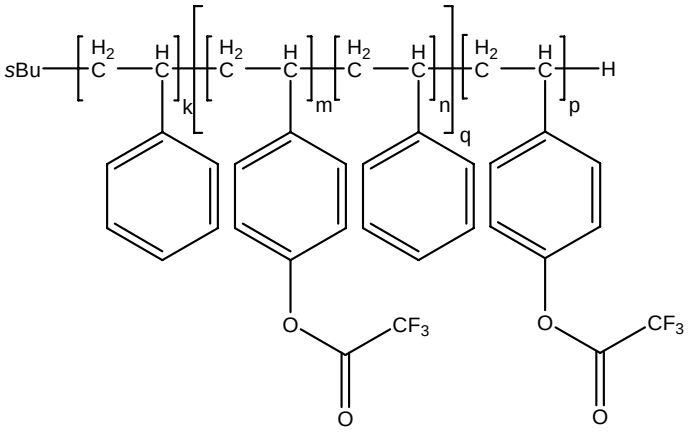

Figure 12. Polystyrene-*block*-poly(*para*-trifluoroacetoxy styrene): PS-*b*-P*p*TFAS.

The hydroxyl moieties in the P*p*HS blocks are considered as functional groups, and therefore polymer-analogous reactions can be performed in order to obtain various multiblock copolymer systems. For example, esterification of the hydroxyl groups using trifluoroacetic anhydride (TFAA) introduces trifluoroacetoxy moieties. In this thesis, the synthesis of

[56] Li, M.; Douki, K.; Goto, K.; Li, X.; Coenjarts, C.; Smilgies, D.M.; Ober, C.K. *Chem. Mater.* **2004**, *16*, 3800.
[57] Landry, C.J.T.; Coltrain, B.K.; Teegarden, D.M.; Long, T.E.; Long, V.K. *Macromolecules* **1996**, *29*, 4712.
[58] Kratochvíl, J.; Šturcová, A.; Sikoro, A.; Dybal, J. *Eur. Polym. J.* **2009**, *45*, 1851.

polystyrene-*block*-poly(*para*-trifluoroacetoxy styrene) (PS-*b*-P*p*TFAS) multiblock copolymers (Figure 12) and their phase behavior will be studied as well. It is believed that self-assembly of these copolymers can be achieved when cooling down from the melt.

2. Experimental

2.1. Materials

Purification of THF and styrene were both performed on a high-vacuum line. Tetrahydrofuran (THF, 99.9 %, Acros Organics) was reacted with *s*BuLi under nitrogen atmosphere, condensed at room temperature and subjected to two freeze-pump-thaw cycles prior to use. Styrene (S, 99 %, Acros Organics) was dried over CaH_2 overnight under nitrogen atmosphere and condensed at room temperature into a flask containing dibutyl magnesium. After stirring overnight under nitrogen atmosphere, a second condensation at room temperature was performed, followed by two freeze-pump-thaw cycles. The monomer was stored under nitrogen at -18°C. 4-*tert*-butoxy styrene (*t*BOS, 99 %, Sigma-Aldrich) was distilled under vacuum from CaH_2, followed by vacuum distillation from dibutyl magnesium. Two freeze-pump-thaw cycles were performed and the monomer was stored under nitrogen at 6 °C. *Sec*-butyl lithium (*s*BuLi, 1.4 M in cyclohexane, Sigma-Aldrich) was used without further purification. Methanol was degassed by nitrogen gas flow. 1,4-Dioxane (99 +%, Acros Organics), hydrochloric acid (HCl, 37 % in water, Merck), trifluoroacetic anhydride (TFAA, 99 +%, Acros Organics), pyridine (99.5 %, Acros Organics) and osmium(VII)-tetroxide (OsO_4, 99.9 +%, Acros Organics) were used as received.

2.2. Characterization

Proton and Carbon-13 nuclear magnetic resonance (^{1}H-NMR and ^{13}C-NMR) spectra were recorded on a 300 MHz Varian VXR at room temperature, using $(CD_3)_2CO$ (deuterated acetone) as solvent unless noted differently.

Attenuated total reflection infrared (ATR-IR) spectrometry was performed at room temperature on a Bruker IFS 88.

Gel permeation chromatography (GPC) was carried out in THF at 25°C (1 mL/min) on a Spectra-Physics AS 1000, equipped with PLGel 5 μ 30 cm mixed-C columns. Universal calibration was applied using a Viscotek H502 viscometer and Shodex RI-71 refractive index detector.

Small-angle X-ray scattering (SAXS) measurements were performed at 25°C and 100°C on a Bruker SAXS with a beam path of 1 m.

Ultrathin microtomed sections (ca. 80 nm) of a solvent-cast block copolymer film (from THF or dioxane) embedded in epoxy resin were placed on copper grids, vapor stained (with OsO_4) and imaged with bright-field transmission electron microscopy (TEM), using a JEOL-1200EX operating at an accelerating voltage of 100 kV.

2.3. Sequential anionic polymerization

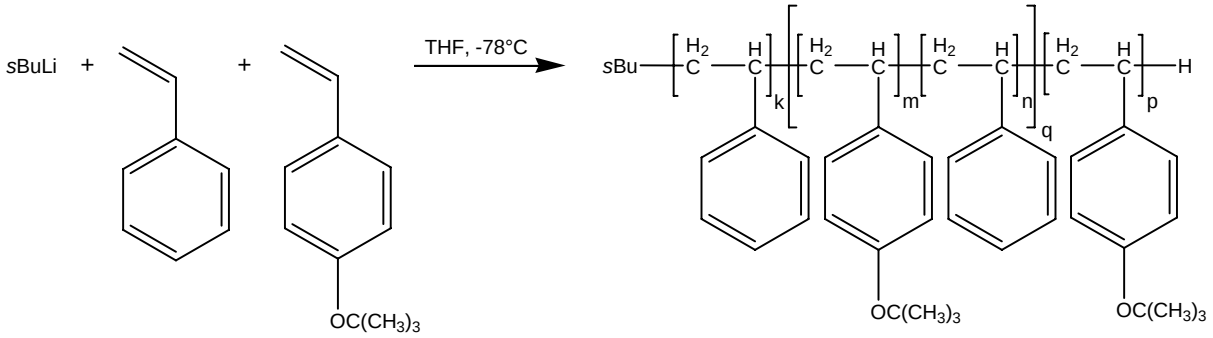

Scheme 4. Synthesis of P(S-*b*-*t*BOS) multiblock copolymers through anionic polymerization

The polystyrene-*block*-poly(*tert*-butoxy styrene) multiblock copolymers were synthesized through sequential anionic polymerization of styrene and *tert*-butoxy styrene on a high vacuum line. The polymerization (Scheme 4) was performed in THF at -78 °C under nitrogen atmosphere, using *sec*-butyl lithium as initiator (Table 1).

Table 1. Living anionic polymerization of PS-*b*-P*t*BOS.

entry	n	N	m	V_{BuLi}[a] (mL)	$V_{S,mid}$[b] (mL)	$V_{S,end}$[c] (mL)	$V_{tBOS,mid}$[d] (mL)	$V_{tBOS,end}$[e] (mL)
1	5	90	2.4	0.05	0.39	0.92	0.55	1.32
2	5	90	3.0	0.05	0.39	0.92	0.55	1.32
3	7	90	2.4	0.05	0.39	1.16	0.55	1.65
4	3	180	3.0	0.05	0.72	1.95	1.02	3.06

[a]Volume of buthyl lithium. [b]Volume of styrene middle blocks. [c]Volume of styrene end blocks. [d]Volume of *tert*-butoxy styrene middle blocks. [e]Volume of *tert*-butoxy styrene end blocks.

400 mL of THF was cooled down to -78 °C and styrene was added via a syringe, followed by *sec*-butyl lithium to initiate the reaction. The reaction mixture turned bright yellow after the addition of *s*BuLi, indicating the presence of anionic species. After reacting for 30 min, 10 mL of the reaction mixture was isolated and precipitated into degassed methanol in order to analyze the degree of polymerization and polydispersity. Subsequently, *tert*-butoxy styrene was added and the mixture was reacted for another 30 min. Alternating, styrene and *t*BOS

were added to obtain the desired multiblock copolymer. The polymerization was terminated by the addition of 1 mL degassed methanol. The mixture turned colorless again, indicating a successful termination.

The reaction mixture was concentrated to ca. 100 mL and precipitated in 1200 mL H_2O. After filtration, the crude product was dried overnight under vacuum at 40 °C. Reprecipitation was performed from a 80 mL $CHCl_3$ solution in 1000 mL methanol, followed by filtration. The obtained white powder was dried under vacuum overnight at 40 °C.

2.4. Hydrolysis

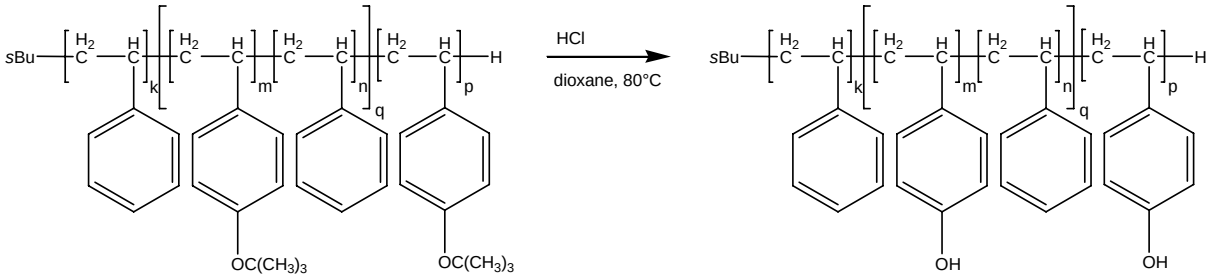

Scheme 5. Conversion of PS-*b*-P*t*BOS to PS-*b*-P*p*HS by hydrolysis.

PS-*b*-P*t*BOS was converted to polystyrene-*block*-poly(*para*-hydroxy styrene) by hydrolysis (Scheme 5).

PS-*b*-P*t*BOS (2.0 g) was dissolved in 75 mL dioxane and 6.0 mL of 37 wt% hydrochloric acid was added. Hydrolysis was carried out overnight at 80 °C under nitrogen atmosphere. The reaction mixture was concentrated to ca. 50 mL and precipitated in 600 mL H_2O. After neutralization with 5 wt% NaOH solution to a pH value of 6, the crude product was filtered and dried overnight under vacuum at 40 °C. The crude product was dissolved in 40 mL THF, reprecipitated in hexanes, filtered and dried under vacuum overnight at 40 °C to obtain a white solid.

2.5. Esterification

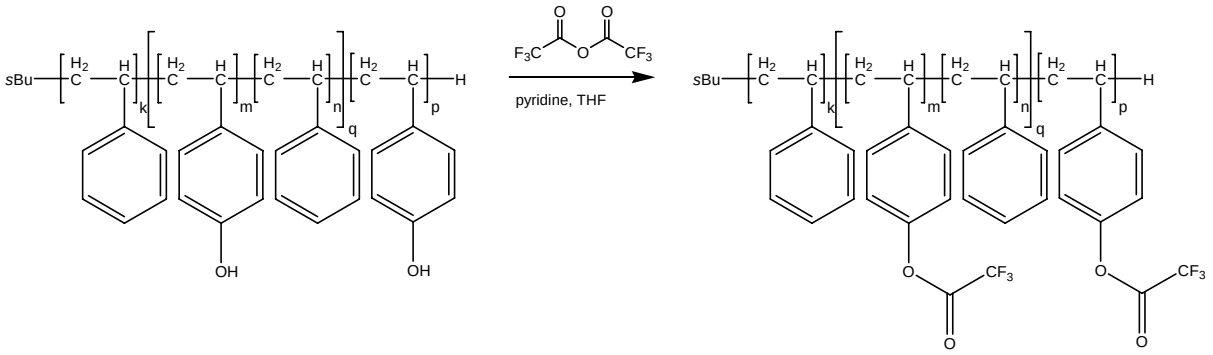

Scheme 6. Conversion of PS-*b*-P*p*HS to PS-*b*-P*p*TFAS by esterification.

PS-*b*-P*p*HS was converted to polystyrene-*block*-poly(*para*-trifluoroacetoxy styrene) by esterification (Scheme 6).

PS-*b*-P*p*HS (0.25 g) was dissolved in 50 mL THF and the solution was cooled with an ice bath. Subsequently, 5 eq of pyridine followed by 3 eq of trifluoroacetic anhydride were slowly added via a syringe. Esterification was carried out overnight under nitrogen atmosphere at room temperature. The reaction mixture was precipitated in 600 mL H_2O. The product was filtered and dried overnight under vacuum at 40 °C to obtain a beige solid.

2.6. Sample preparation

Multiblock copolymer was dissolved in THF or dioxane (1.0 and 1.5 wt%) and a film was cast from solution. Solvent was slowly evaporated, and the sample was annealed in a saturated vapor for one week. Subsequently, the film was placed in an oven for 30 minutes at 100 °C.

In order to prepare TEM samples, a piece of block copolymer film was embedded in epoxy resin and cured at 40 °C overnight. Ultrathin sections were microtomed to a thickness of about 80 nm using a diamond knife. These microtomed sections were floated on water and placed on copper grids. In addition, vapor staining with OsO_4 was applied for 2 days to obtain contrast during TEM measurements.

3. Results and Discussion

3.1. Synthesis and characterization of multiblock copolymers

3.1.1. Sequential anionic polymerization

PS-*b*-P*t*BOS multiblock copolymers with two-length-scale molecular architecture were prepared through a multistep sequential anionic polymerization. The architecture of these copolymers is described by the parameters introduced by Smirnova *et al.*[34,35] (*n*, *N*, *m*), as mentioned in the introduction. One octablock copolymer (*n* = 3), two dodecablock copolymers (*n* = 5) and one hexadecablock copolymer (*n* = 7) were successfully synthesized. The corresponding architecture parameters, together with the results following from GPC analysis, are depicted in Table 2. Both NMR and IR data will be discussed in the next section, combined with the results from hydrolysis.

Table 2. Molecular weight (distribution) of PS-*b*-P*t*BOS.

entry	n	N	m	$M_{n,prec}$ [a] ($kg \cdot mol^{-1}$)	$[I]_0$ [b] (μmol)	M_n [c] ($kg \cdot mol^{-1}$)	PDI [d]
1	5	90	2.4	14.7	57.1	105.8	1.28
2	5	90	3.0	22.5	46.7	143.9	1.18
3	7	90	2.4	22.0	38.3	203.1	1.24
4	3	180	3.0	26.0	75.0	141.9	1.25

[a]Molecular weight of precursor (block I) as determined by GPC. [b]Initial initiator concentration as calculated from GPC data. [c]Molecular weight of copolymer as determined by GPC. [d]Polydispersity as determined by GPC.

The molar mass of the polystyrene precursors, isolated from the reaction mixture, directly corresponds to the final molecular weight of the multiblock copolymers, as designed. This represents the living nature of the anionic polymerization: the polymer chains retain their ability to propagate and grow to a desired size, since the degree of termination and chain transfer is negligible.

The initial initiator concentration of *sec*-butyl lithium was determined from the precursor molecular weight and the mass of added styrene monomer, since the degree of polymerization is equal to the ratio between initial monomer and initial initiator concentration for monofunctional initiators (Equation 3). Naturally, higher initiator concentrations result in lower molecular weights and vice versa. For example, the expected initial initiator concentration of polymerization **1** was 70 μmol, where the actual value is calculated to be

57.1 µmol (Table 2). As a consequence, the molecular weight as determined from GPC is 105.8 kg·mol^{-1} instead of 74 kg·mol^{-1}.

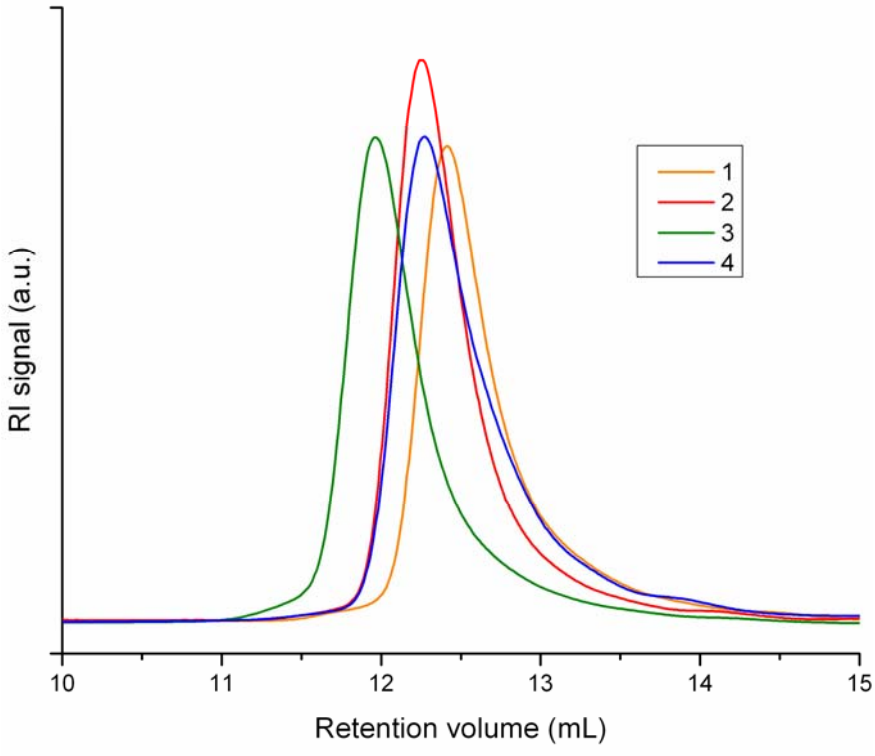

Figure 13. (a) GPC chromatograms of four multiblock copolymers. (1) Dodecablock (m = 2.4), (2) dodecablock (m = 3.0), (3) hexadecablock, (4) octablock.

Figure 13 compares GPC chromatograms of the synthesized copolymers, all indicating a narrow molecular weight distribution. Polydispersity index (PDI) values, determined by universal calibration, vary between 1.18 and 1.28 (Table 2). Although lower polydispersities are reported for comparable multiblock copolymer products synthesized through living anionic polymerization[28,29,30], the obtained molecular weight distributions are still reasonably narrow compared to dispersities of block copolymers synthesized through other polymerization techniques such as controlled radical polymerization, and therefore support the controlled nature of the reaction. Furthermore, GPC calibration samples indicated some peak broadening, supposedly due to slightly damaged columns, resulting in higher polydispersities as well.

The elution diagram of styrene precursor **1** is showing a high molecular weight shoulder (Appendix 1). This trend is observed for all styrene precursors, and indicates oxidative coupling of polymer chains ends resulting from precipitation of the isolated fraction in

methanol. In addition, the GPC chromatogram of a premature terminated multiblock copolymer is also depicted in Appendix 1. During polymerization, the bright yellow reaction mixture turned colorless after addition of the fourth block (*t*BOS). This indicates disappearance of active anionic species and thus termination of the living chains ends, supposedly due to the presence of some contamination in the system. Not surprisingly, a broader molecular weight distribution was obtained with a PDI value of 1.44. The elution diagram depicts a non-uniform distribution, and the molecular weight was determined to be 89.5 $kg \cdot mol^{-1}$. From now on, this special tetrablock copolymer will be referred as copolymer **5**, and the phase behavior was studied together with the other well-defined copolymers.

3.1.2. Hydrolysis

In order to obtain monodispers poly(*para*-hydroxy styrene) blocks, protection of the phenol groups prior to anionic polymerization is required, to avoid termination of the living chain ends. As discussed above, *tert*-butyl ether was introduced as protection group, since both styrene and tert-butoxy styrene are able to polymerize subsequently. Furthermore, *t*BOS is commercially available and can be hydrolyzed under relatively mild conditions. Indeed, for the first time PS-*b*-P*p*HS multiblock copolymers (with two-length-scale architecture) were successfully prepared through acidic cleavage of the *tert*-butoxy moieties in the PS-*b*-*t*BOS copolymers.

The corresponding FTIR spectrum of dodecablock copolymer **1** after hydrolysis (Figure 14a) displays a broad peak at 3318 cm^{-1} that is initially absent (Figure 14b). This indicates the successful conversion from *tert*-butoxy to hydroxyl groups.

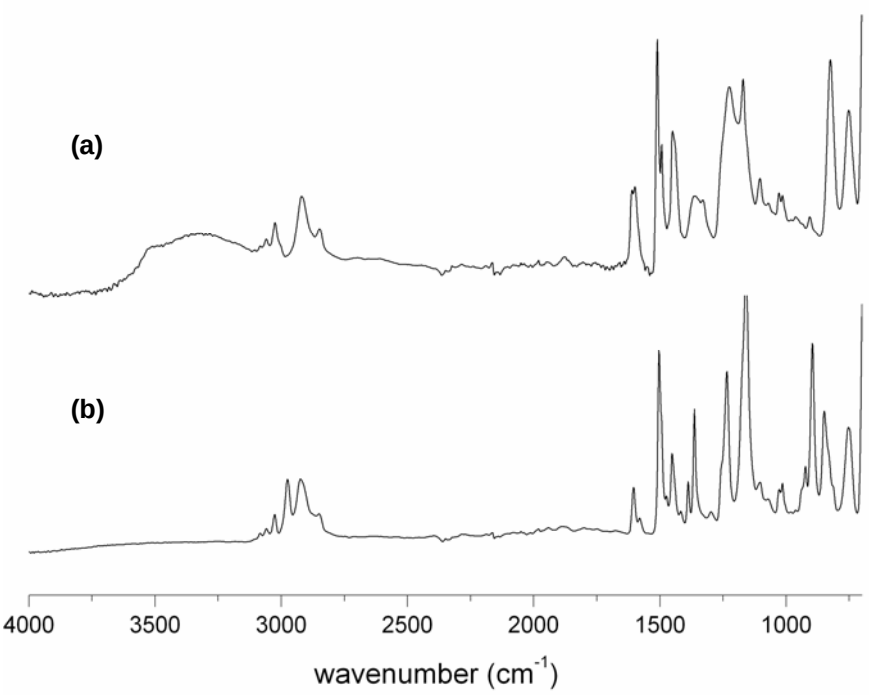

Figure 14. (a) FTIR spectrum of PS-*b*-P*p*HS dodecablock copolymer after hydrolysis. (b) FTIR spectrum of initial PS-*b*-P*t*BOS dodecablock copolymer.

Hydrolysis was also studied by NMR spectroscopy. The ^{1}H-NMR spectra of dodecablock copolymer **1** recorded before and after acidic cleavage are displayed in Figure 15a,b. The large chemical shift around 1.31 ppm, corresponding to the *tert*-butyl protons in the initial PS-*b*-*t*BOS copolymer, completely disappears in the spectrum of the deprotected multiblock copolymer. Absence of this signal indicates complete conversion of hydrolysis. Moreover, a broad peak located around 8.02 ppm (highlighted in red), corresponding to phenol protons, appears after the acidic cleavage.

In addition, ^{13}C-NMR spectra of copolymer **1** recorded before and after deprotection were recorded (Figure 15c,d). The signal located around 77 ppm (highlighted in red), corresponding to the quaternary carbon atoms of tert-butyl groups in *t*BOS, entirely disappears in the spectrum of the hydrolyzed copolymer, again proving the successful conversion of acidic cleavage.

Similar trends were observed in the recorded FTIR and NMR spectra of multiblock copolymers **2**, **3** and **4**, as well as in the literature[15,16].

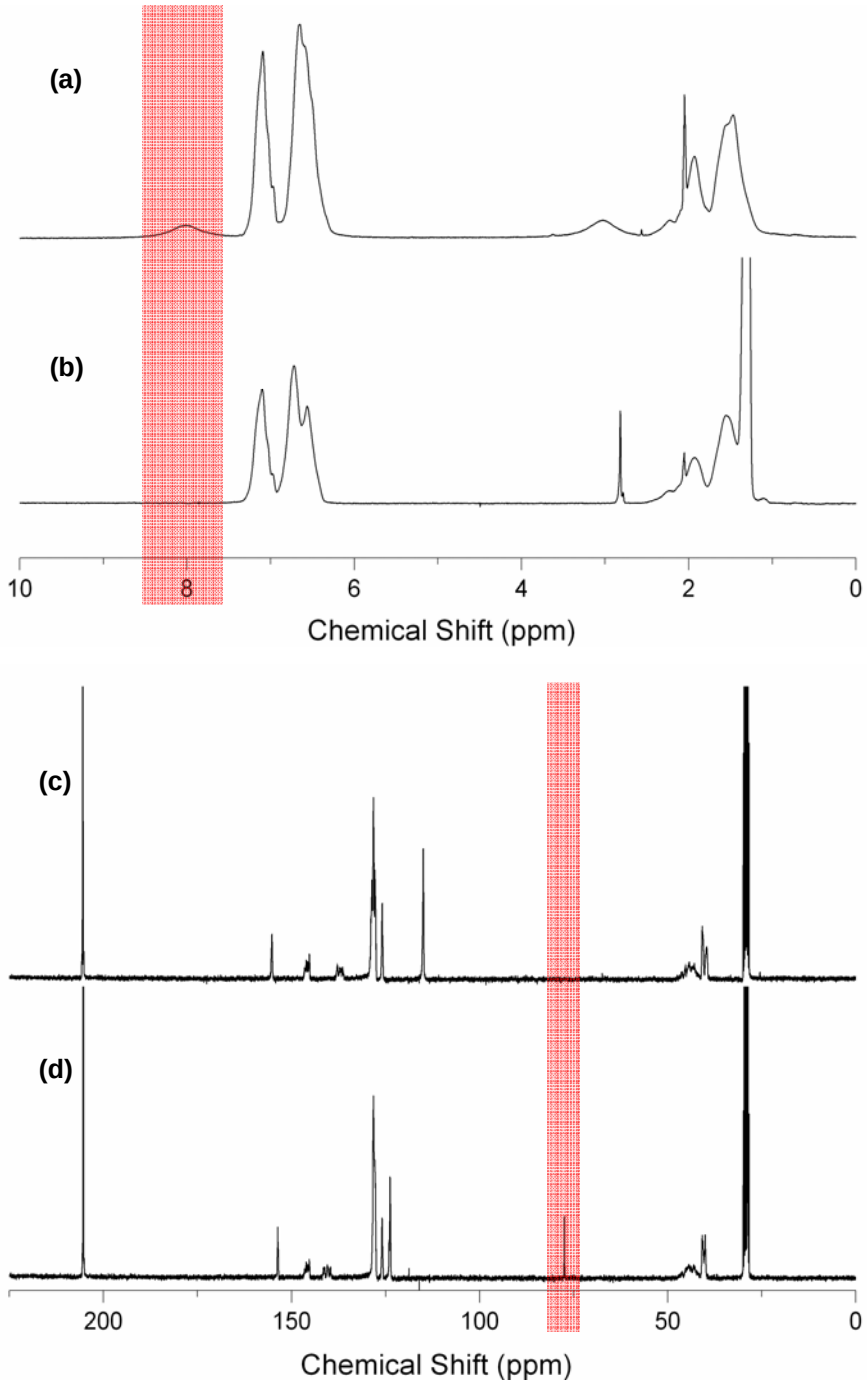

Figure 15. (a) ^{1}H-NMR spectrum of PS-*b*-P*p*HS dodecablock copolymer after hydrolysis. (b) ^{1}H-NMR spectrum of initial PS-*b*-P*t*BOS dodecablock copolymer. (c) ^{13}C-NMR spectrum of PS-*b*-P*p*HS dodecablock copolymer after hydrolysis. (d) ^{13}C-NMR spectrum of initial PS-*b*-P*t*BOS dodecablock

Composition of the PS-*b*-P*p*HS copolymers was determined using the relative intensities of the aromatic protons of styrene and *para*-hydroxy styrene (6.1-7.4 ppm), and for multiblock copolymer **1** the spectrum revealed a composition of 47 mol% P*p*HS segments corresponding

to 51 wt%, as designed. Comparable weight fractions are determined for the other three multiblock copolymers (Table 3).

Table 3. Composition of PS-*b*-P*p*HS multiblock copolymers.

entry	n	N	m	f^a (mol%)	f^b (wt%)
1	5	90	2.4	47	50
2	5	90	3.0	45	48
3	7	90	2.4	46	50
4	3	179	3.0	43	47

[a,b]Composition of *p*HS as determined from ^{1}H-NMR spectra.

3.1.3. Esterification

To approach the theoretical model about phase behavior of multiblock copolymers proposed by Smirnova *et al.*[34,35] as close as possible, self-assembly of copolymers has to be achieved through cooling down from the melt. Since PS-*b*-P*p*HS is not suitable for this purpose (solvent-casting is applied instead), an additional copolymer system is desired in order to investigate the theoretical predictions. Therefore, polystyrene-*block*-poly(*para*-trifluoroacetoxy styrene) multiblock copolymers were prepared through esterification of phenol moieties in the PS-*b*-P*p*HS copolymers.

Esterification was applied on PS-*b*-P*p*HS multiblock copolymer **1** and **3**. The ^{1}H-NMR spectrum of dodecablock copolymer **1** after esterification is displayed in Figure 16b. The broad peak located around 8.02 ppm and corresponding to the hydroxyl protons is disappeared in this spectrum recorded directly after precipitation, indicating the conversion from hydroxyl to ester groups.

However, the PS-*b*-P*p*TFAS copolymer product seems to be unstable according to the ^{1}H-NMR spectrum of the same compound recorded two weeks later, showing the presence of phenol groups (Figure 16a). Similar trends were observed for hexadecablock copolymer **3**. Supposedly, the ester moieties undergo UV radiation induced photo-Fries rearrangement. This photo-induced reaction was previously observed for poly(*para*-acetoxystyrene), forming *ortho*-hydroxy keton moieties[59]. Due to this undesired conversion, the glass transition cannot be reached and as a consequence, cooling down from the melt in order to obtain self-assembly is not applicable. In order to still investigate the phase behavior of this particular system, solvent-cast copolymer films were prepared from THF solution.

[59] Fréchet, J.M.J.; Tessier, T.G.; Wilson, C.G.; Ito, H. *Macromolecules* **1985**, *18*, 317.

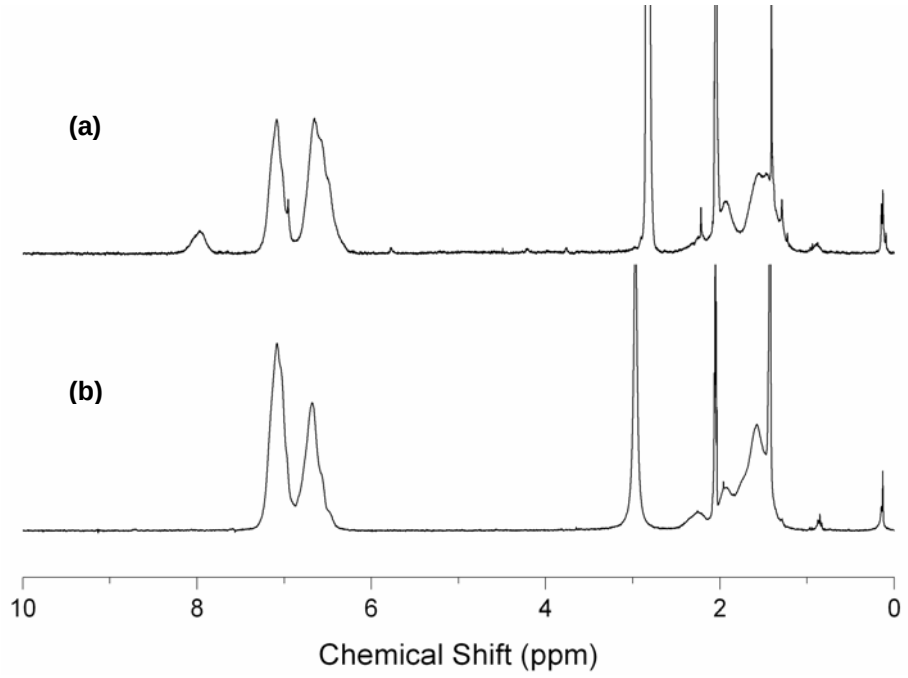

Figure 16. (a) ^{1}H-NMR spectrum of PS-*b*-P*p*TFAS dodecablock copolymer recorded after two weeks. (b) ^{1}H-NMR spectrum of PS-*b*-P*p*TFAS dodecablock copolymer recorded directly after precipitation.

3.2. Multiblock copolymer phase behavior

To study the microphase behavior of PS-*b*-P*p*HS multiblock copolymers with a two-length-scale architecture, solvent-cast block copolymer films were prepared and the self-assembled nanostructure in these films was investigated by small-angle X-ray scattering and transmission electron microscopy. As explained above, cooling down from the melt in order to obtain self-organization was not applicable within this system, since the glass transition of P*p*HS blocks is not reached before condensation cross-linking occurs. Therefore solvent-casting from THF or dioxane solution was applied instead. After preparing ultrathin microtomed sections of the copolymer films embedded in epoxy resin, vapor staining was applied using osmium tetroxide. As explained in the introduction, OsO_4 selectively stains alcohols in the presence of aromatics, i.e. osmium tetroxide will selectively stain the P*p*HS blocks. Therefore, OsO_4 is thought to be a useful staining agent to reveal the block copolymer morphology.

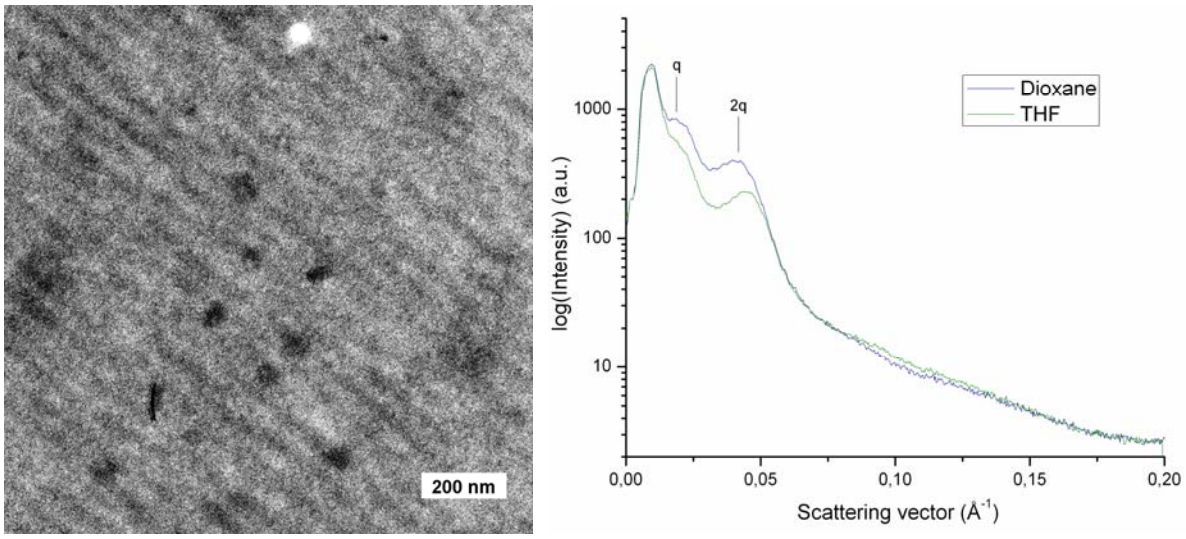

Figure 17. (left) TEM image of PS-*b*-P*p*HS dodecablock copolymer **1**, solvent-cast from THF and stained with OsO_4. (right) SAXS intensity profiles of PS-*b*-P*t*BOS dodecablock copolymer **1**, solvent-cast from THF and dioxane.

Figure 17 displays a TEM image representing the nanostructure of dodecablock copolymer **1** together with the corresponding SAXS pattern. The scattering profile of the block copolymer film solvent-cast from dioxane represents a lamellar morphology, since integer ordered peaks are observed up to the second-order (Equation 8). The corresponding 2D SAXS pattern is depicted in Appendix 2. As expected, diffracted peak positions in the pattern of the copolymer solvent-cast from THF are similar. The repeating distance is determined to be 33 nm (Table 4) by applying Bragg's condition (Equation 7). Corresponding to the SAXS profile, the obtained transmission electron micrograph is indeed revealing a lamellar one-length scale nanostructure. Although the lateral order of lamellae is promising, the degree of microphase separation is limited. Probably, the low extent of phase separation is induced by the small chain length of the middle diblock units (N = 90). Together with the Flory-Huggins interaction parameter $\chi_{S,pHS}$ which is assumed to be 0.25[57], this results in a relatively low value of $\chi \cdot N \approx 23$ for the middle diblocks. Supposedly, the observed lamellar structure is therefore arising from microphase separation of the larger end blocks.

Similar results are obtained from TEM and SAXS analysis of dodecablock copolymer **2** (Figure 18), solvent-casted from THF solution. The scattering profile is showing integer numbered peaks up to second-order, revealing a lamellar nanostructure as well. According to the first-order peak, the period is equal to 40 nm (Table 4). The increased repeating unit corresponds with the longer end blocks of copolymer **2** compared to **1**, as designed. The corresponding TEM image is depicting a lamellar morphology as well. Again, the limited

degree of microphase separation is indicating the mixing of short middle diblock chains, and the nanostructure arises from phase segregated end blocks.

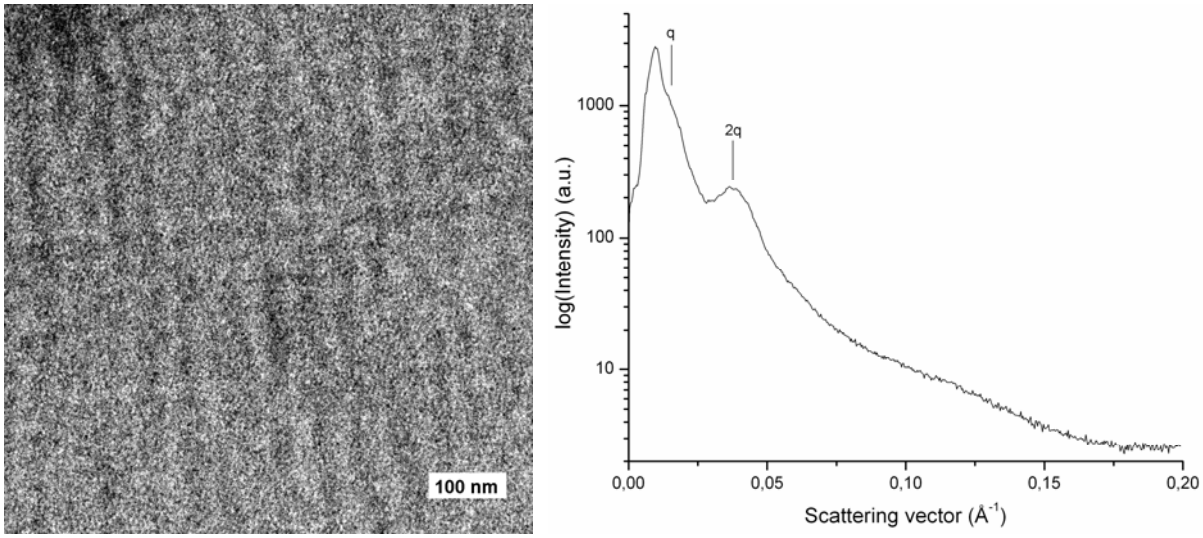

Figure 18. (left) TEM image of PS-*b*-P*p*HS dodecablock copolymer **2**, solvent-cast from THF and stained with OsO_4. (right) Corresponding SAXS intensity profile.

The SAXS profile of hexadecablock copolymer **3** (Figure 19) is depicting only one diffraction peak. Therefore, the morphology of the nanostructure cannot be determined. Moreover, from the transmission electron micrograph it is difficult to distinguish phase segregated microdomains. The appearance of this single diffraction peak however implies ordering at the nanoscale. The repeating distance of this ordering is determined to be 17 nm (Table 4) according to Bragg's condition. As explained in the introduction, D decreases with an increasing number of blocks n. Indeed, the period is significantly smaller compared to the repeating units determined for copolymer **1** and **2**, due to the increased number of middle diblock units (n = 7). In combination with the small value of $\chi \cdot N$, this results in a low degree of phase separation.

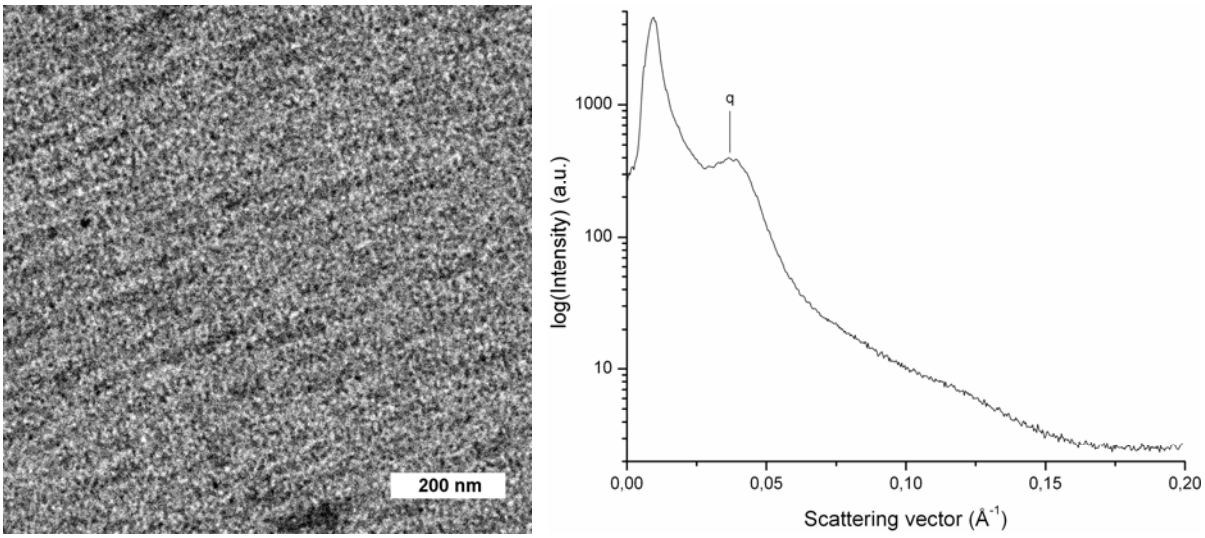

Figure 19. (left) TEM image of PS-*b*-P*p*HS hexadecablock copolymer **3**, solvent-cast from THF and stained with OsO_4. (right) Corresponding SAXS intensity profile.

As mentioned in the previous section, the synthesized PS-*b*-P*p*TFAS copolymers are unstable and cooling down from the melt in order to obtain self-organization is not applicable, since the glass transition cannot be reached. However, the phase behavior of this system was still investigated by preparing solvent-cast copolymer films of the converted dodecablock copolymer **1** and hexadecablock copolymer **3**, and the corresponding TEM images and SAXS patterns are displayed in Appendix **3**. The transmission electron micrographs indicate that the degree of microphase separation is still limited and thus not improved. SAXS intensity profiles are similar to the profiles obtained for the corresponding PS-*b*-P*p*HS copolymers. The scattering pattern of converted copolymer **1** is revealing a lamellar morphology, and the repeating distance of the structure was calculated to be 29 nm according to Bragg's condition. In addition, a repeating unit of 15 nm was determined for the nanostructure of converted copolymer **3**.

Table 4. Repeating unit in PS-*b*-P*p*HS multiblock copolymer nanostructures.

entry	n	N	m	D[a] (nm)
1	5	90	2.4	33
2	5	90	3.0	40
3	7	90	2.4	17
4	3	180	3.0	44[b]

[a]Repeating distance as determined from SAXS intensity profiles. [b]Repeating distance of two-length-scale nanostructure.

To study the self-assembly of octablock copolymer **5** extensively, both 1.0 wt% and 1.5 wt% block copolymer solutions in THF were prepared and solvent-casting was applied. Both TEM image and SAXS intensity profile of the film solvent-cast from 1.0 wt% solution are displayed in Appendix 4. The scattering pattern implies a lamellar nanostructure, since integer ordered diffracted peak are observed up to second-order. From the first-order peak, a repeating unit of 25 nm was calculated. On the other hand, the TEM image is revealing a nanostructure with small domains consisting of lamellae and spheres.

In Figure 20a-d, four transmission electron micrographs of the copolymer film solvent-cast from 1.5 wt% THF solution are depicted. Clearly, a unique two-length-scale lamellar morphology with double periodicity is observed. The structure includes one thick lamellar domain of polystyrene (*light*), one thick lamellar domain of poly(para-hydroxy styrene) (*dark*), and two thin lamellae in between, consisting of PS (*light*) and P*p*HS (*dark*). Contrast results from the selective staining of the hydroxyl moieties in P*p*HS with osmium tetroxide. The greatly improved degree of microphase separation compared to that of copolymers **1**, **2** and **3** is probably induced by the larger chain length of the middle diblock units ($N = 180$): the value of $\chi \cdot N$ for the center diblocks is increased to 45.

The observed hierarchical lamellar-in-lamellar nanostructure is in excellent agreement with the two-length-scale multiblock copolymer architecture. The thick lamellar layers arise from the large end blocks, and the smaller middle diblock units self-assemble in the two thin lamellae in between. Two possible conformations of the octablock copolymer are presented in Figure 21a.

The two-length-scale morphology is clustered in local domains with typical length scales of 1-2 μm (Figure 20a), i.e. the degree of long-range order is limited. In addition, a different nanostructure is observed, similar to the structure in the copolymer film solvent-cast from 1 wt% THF solution (Appendix 3). Indeed, the SAXS intensity profile (Figure 20f) depicts an additional scattering peak at $q = 0.25$ nm^{-1}, corresponding to a repeating distance of 25 nm. Therefore, it is believed that this diffraction peak arises from the alternative structure observed in the TEM images. The other peaks are representing the first- and third-order diffractions of the lamellar-in-lamellar nanostructure, and the corresponding repeating distance is 44 nm (Table 4) according to Bragg's condition. Due to symmetry, the second-order scattering peak is absent, which is supported by the 2D Fourier transform (Figure 20e) of the lamellar-in-lamellar nanostructure depicted in Figure 20c.

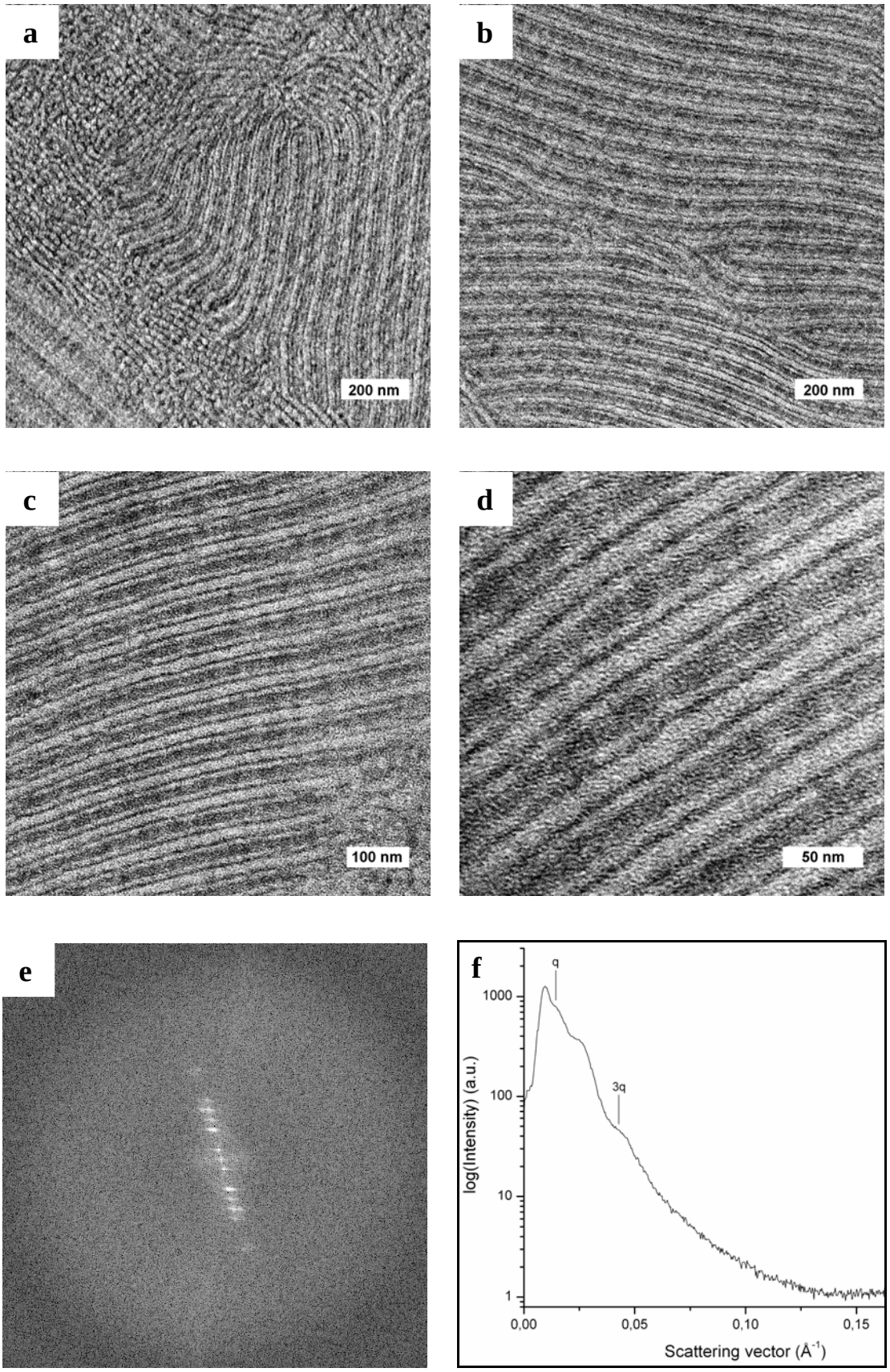

Figure 20. (a-d) TEM images of PS-*b*-P*p*HS octablock copolymer **4**, solvent-cast from 1.5 wt% THF solution and stained with OsO_4. (e) Corresponding 2D Fourier transform. (f) Corresponding SAXS intensity profile.

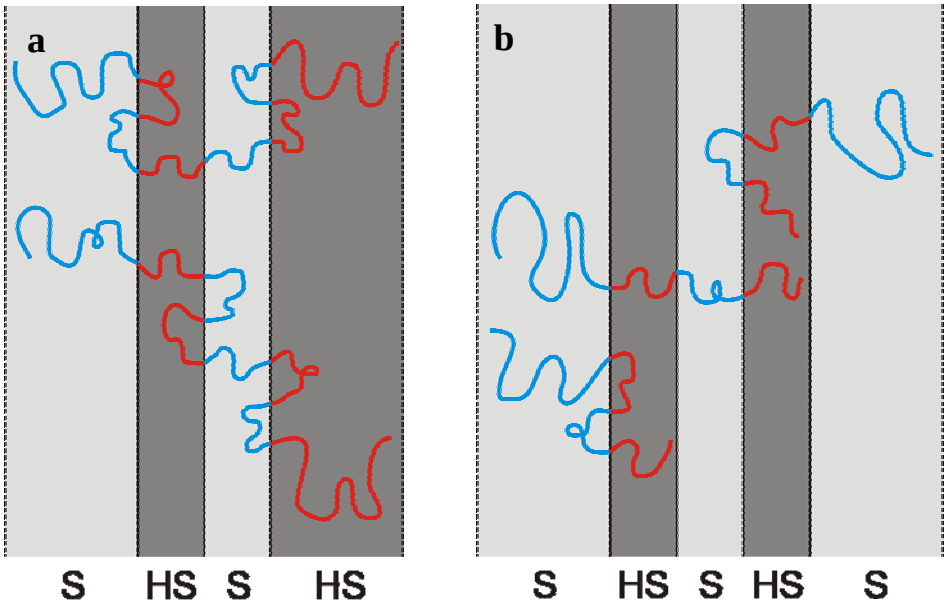

Figure 21. (a) Two possible conformations of PS-*b*-P*p*HS octablock copolymer **4** in the hierarchical lamellar-in-lamellar structure. (b) Three possible conformations of PS-*b*-P*p*HS tetrablock copolymer **5** in the hierarchical lamellar-in-lamellar structure.

From the transmission electron micrograph of tetrablock copolymer **5** (Figure 22), another two-length-scale lamellar nanostructure with multiple periodicity is observed. This hierarchical morphology consists of thick lamellar domains of polystyrene (*light*) with three thin lamellar layers of alternating P*p*HS (*dark*) and PS (*light*) in between. The lamellar-in-lamellar structure is in excellent agreement with the two-length-scale architecture of the tetrablock copolymer. The thick lamellae arise from the long end chain, while the three short blocks self-assemble in three thin lamellar layers. Three possible conformations of the tetrablock copolymer are presented in Figure 21b.

The two-length-scale nanostructure is observed in local domains with typical length scales of 0.5-1 μm. The size of these local domains is relatively small, supposedly due to the broader molecular weight distribution of this premature terminated copolymer compared to the polydispersity of octablock copolymer **4** (Table 2).

The corresponding SAXS intensity profile is showing first- and fourth-order diffraction peaks, and the repeating unit is determined to be 40 nm. In addition, an alternative scattering peak at q = 0.40 nm^{-1} (D = 16 nm) is observed. This diffraction probably arises from an alternative self-assembled nanostructure present in the same block copolymer system.

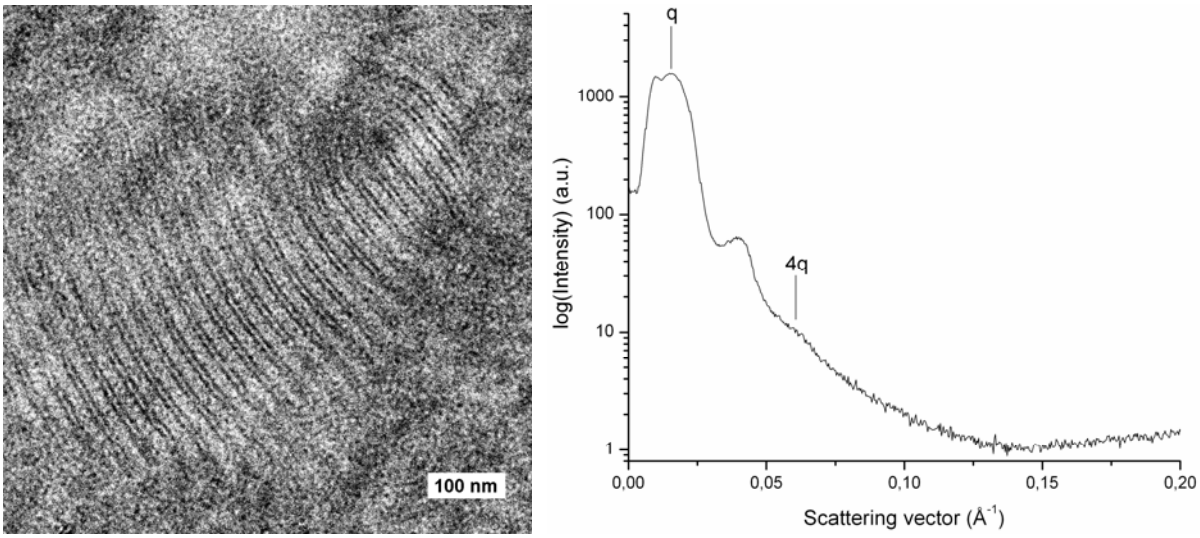

Figure 22. (left) TEM image of PS-*b*-P*p*HS tetrablock copolymer **5**, solvent-cast from THF and stained with OsO_4. (right) Corresponding SAXS intensity profile.

4. Conclusions

Polystyrene-*block*-poly(*tert*-butoxy styrene) multiblock copolymers with two-length-scale molecular architectures, as described theoretically by Smirnova *et al.*, were successfully synthesized through sequential living anionic polymerization in THF at -78 °C with *sec*-butyl lithium as initiator. The copolymers are composed of two large end blocks and multiple short diblock units at the center: PS-*b*-(P*t*BOS-*b*-PS)$_n$-*b*-P*t*BOS. Narrow molecular weight distributions with polydispersities between 1.18 and 1.28 were determined from GPC measurements. Acidic cleavage of *tert*-butoxy groups resulted in the first successful formation of polystyrene-*block*-poly(*para*-hydroxy styrene) multiblock copolymers with two-length-scale architecture.

Phase behavior of these multiblock copolymers was studied by transmission electron microscopy and small-angle X-ray scattering, analyzing solvent-cast films from dioxane and THF. Dodecablock copolymer **1** revealed a lamellar morphology with a period of 33 nm. The limited degree of microphase separation is probably induced by the short chain length of the middle diblock units (N = 90), and the lamellar structure is therefore thought to arise from phase separation of the larger end chains. Similar results were obtained for dodecablock copolymer **2**. The repeating distance of 40 nm is in agreement with the larger end blocks of this multiblock copolymer. From TEM analysis of hexadecablock copolymer **3**, no phase segregated microdomains were distinguished. The large number of middle diblock units (n = 7) in combination with their short chain length (N = 90) resulted in a low degree of phase separation. The corresponding SAXS pattern however depicted one diffraction peak, indicating ordering with a repeating unit of 17 nm.

Esterification of PS-*b*-P*p*HS was performed to obtain polystyrene-*block*-poly(*para*-trifluoroacetoxy styrene) multiblock copolymers. It was believed that self-assembly of these copolymers could be achieved when cooling down from the melt. Unfortunately, the PS-*b*-P*p*TFAS copolymers were not stable according to ^{1}H-NMR analysis. In order to still investigate the phase behavior of this system, solvent-cast copolymer films were prepared from THF solution. The degree of microphase separation was not improved compared to the PS-*b*-P*p*HS copolymers and similar repeating units were determined.

TEM images of octablock copolymer **4** displayed a unique two-length-scale lamellar nanostructure with double periodicity. The morphology includes one thick lamellar domain of PS, another thick lamellar domain of P*p*HS, and two thin lamellae of PS and P*p*HS in between. This new hierarchical lamellar-in-lamellar structure is in excellent agreement with

the two-length-scale multiblock copolymer architecture. The greatly improved degree of microphase separation is induced by the larger chain length of the middle diblock units (N = 180). The period of the large length scale was determined to be 44 nm. Long-range ordering of the two-length-scale morphology is limited, since local domains of 1-2 μm were observed.

A different lamellar-in-lamellar structure was observed for tetrablock copolymer **5**. This hierarchical morphology consists of thick lamellar domains of PS with three thin lamellar layers of alternating P*p*HS and PS in between. The nanostructure, with a large length scale period of 40 nm, is in excellent agreement with the two-length-scale architecture of the copolymer. The degree of long-range order is relatively low (local domains of 0.5-1 μm), due to the higher polydispersity of this premature terminated tetrablock copolymer.

It is expected that multiblock copolymers with longer block lengths can stimulate long-range ordering of the observed lamellar-in-lamellar morphologies. Therefore, additional sequential anionic polymerizations may be employed in the near future. Furthermore, a reliable determination of the Flory-Huggins interaction parameter is desired, to improve the understanding of the phase behavior of this particular system. In addition, alternative polymer-analogous reactions may be performed to obtain a multiblock copolymer system that enables self-organization through cooling down from the melt.

5. Acknowledgements

First of all, I would like to thank my supervisor Martin Faber for his help and support during my day-to-day synthesis at the polymer chemistry department of the University of Groningen. I also greatly acknowledge Prof. dr. Gerrit ten Brinke and Prof. dr. Katja Loos for their guidance and advice considering my project. Ing. Joop Vorenkamp is thanked for the assistance with GPC measurements, and Dr. Evgeny Polushkin for his help with the SAXS experiments. I would also like to acknowledge Dr. Mark Stuart for the extensive training on TEM. Special thanks to Ivana Vukovic for the useful discussions we had regarding my research. To conclude, I thank all the people from the polymer chemistry department of the University of Groningen, for creating such a pleasant atmosphere to perform my research.

6. Appendix

1. GPC chromatograms of styrene precursor **1** and PS-*b*-P*t*BOS tetrablock copolymer **5**.

2. 2D SAXS pattern of PS-*b*-P*p*HS dodecablock copolymer **1**.

3. TEM image and SAXS intensity profile of PS-*b*-P*p*TFAS dodecablock copolymer **1** and PS-*b*-P*p*TFAS hexadecablock copolymer **3**.

4. TEM image and SAXS intensity profile of PS-*b*-P*p*HS octablock copolymer **4**.

Appendix 1. GPC chromatograms of (a) styrene precursor **1** and (b) PS-*b*-P*t*BOS tetrablock copolymer **5**.

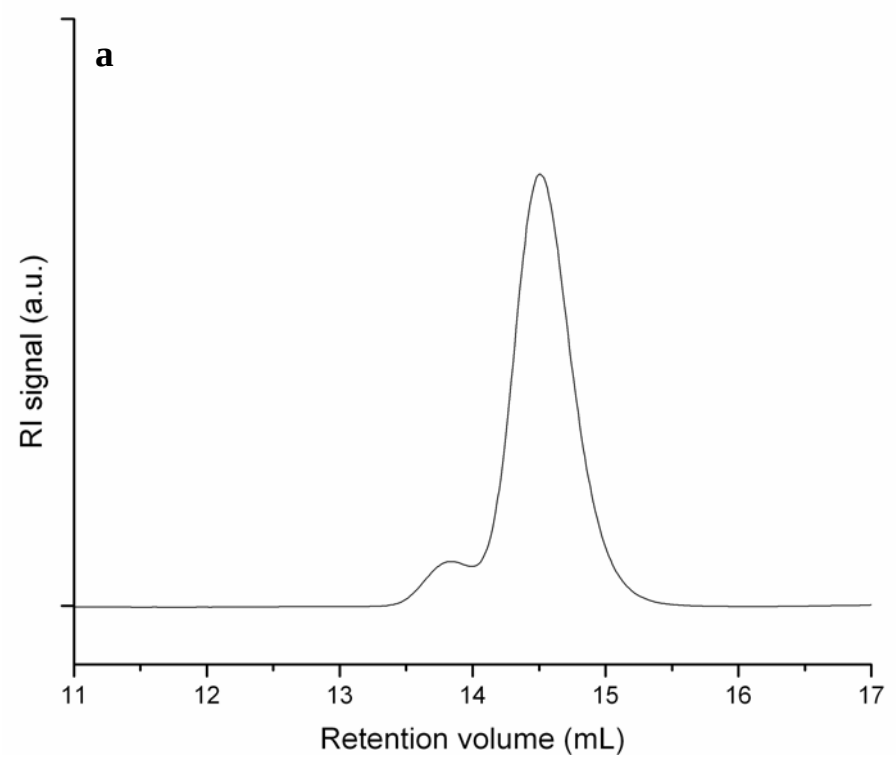

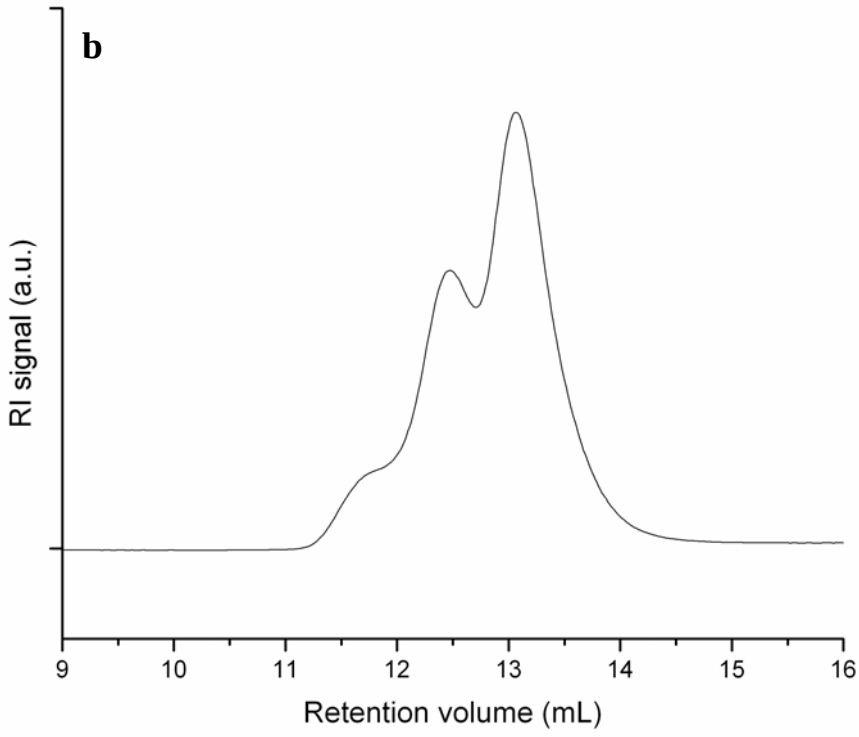

Appendix 2. 2D SAXS pattern of PS-*b*-P*p*HS dodecablock copolymer **1**.

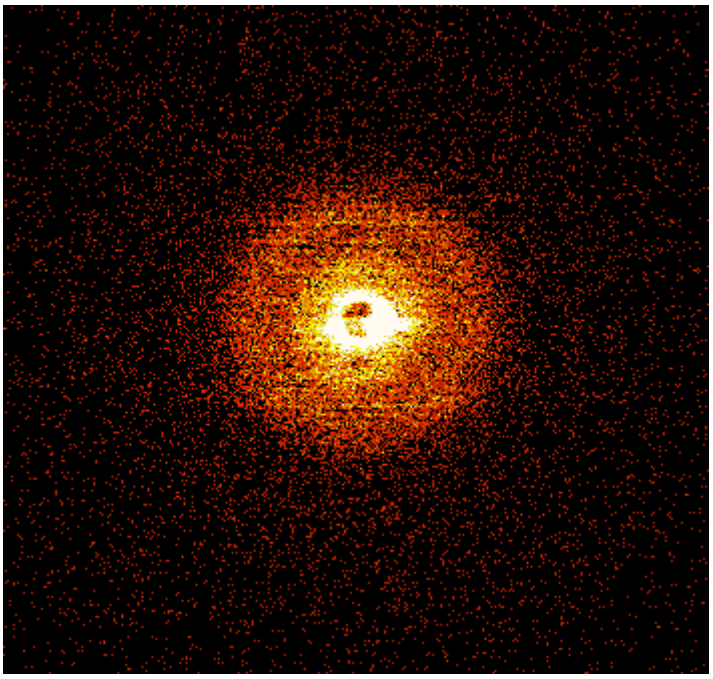

Appendix 3. TEM image and SAXS intensity profile of (a) PS-*b*-P*p*TFAS dodecablock copolymer **1** and (b) PS-*b*-P*p*TFAS hexadecablock copolymer **3**, solvent-cast from THF and stained with OsO4.

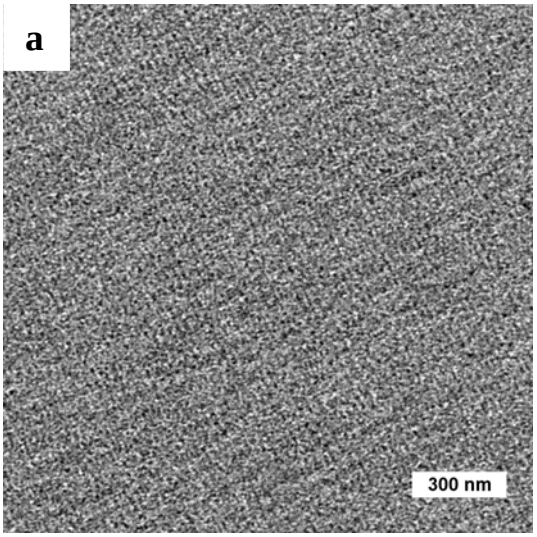

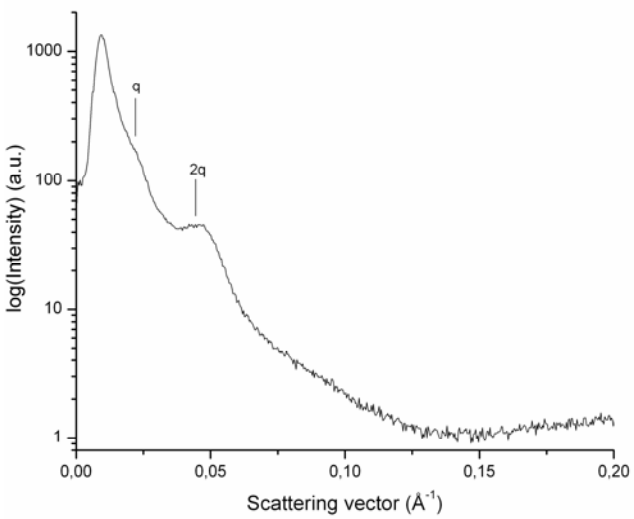

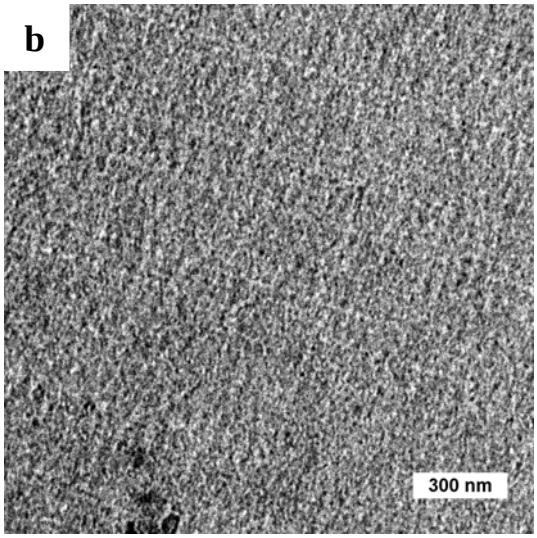

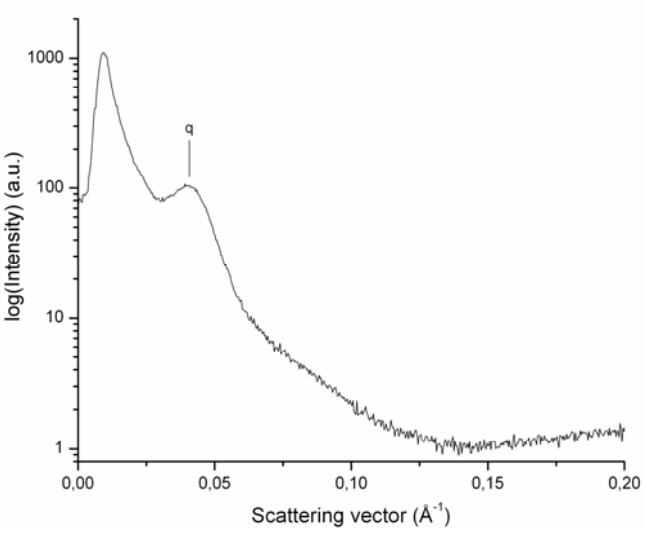

Appendix 4. TEM image and SAXS intensity profile of PS-*b*-P*p*HS octablock copolymer **4**, solvent-cast from 1.0 wt% THF solution and stained with OsO_4.